

In: Strontium Titanate
Editors: A. Tkach and P. Vilarinho

ISBN: 978-1-53615-437-5
© 2019 Nova Science Publishers, Inc.

Chapter 6

**EFFECT OF BISMUTH DOPING ON THE
PROPERTIES OF STRONTIUM TITANATE
THIN FILMS**

Olena Okhay^{*}, *Alexander Tkach* and *Paula M. Vilarinho*
CICECO – Aveiro Institute of Materials, Department of Materials and
Ceramic Engineering. University of Aveiro, Aveiro, Portugal

ABSTRACT

Strontium titanate-based materials with ferroelectric or relaxor-like properties have drawn vast attention for research and wide range of applications in different areas. This chapter summarises firstly the electrical behaviour of Bi-doped strontium titanate ceramics, where three relaxation modes, related to individual hopping of off-centre Bi ions with and without oxygen vacancies nearby, as well as to their collective polar cluster reversal, are induced by Bi doping. Then, the structural and microstructural properties of sol-gel derived $\text{Sr}_{1-1.5x}\text{Bi}_x\text{TiO}_3$ films are reported, revealing enlarged lattice parameter and film roughness with increasing Bi content. Dielectric response of these films demonstrates that,

^{*} Corresponding Author's E-mail: olena@ua.pt.

besides the oxygen vacancy related mode, only two polar relaxation modes exist in the temperature range of 10-300 K. Polarisation versus *ac* electric field hysteresis response of $\text{Sr}_{1-1.5x}\text{Bi}_x\text{TiO}_3$ films confirms the low-temperature polar state induced by Bi doping in strontium titanate (STO) films. Results on the dielectric permittivity versus *dc* electric field indicate that moderately Bi-doped STO films can be considered as a promising material for tunable device applications, due to their high values of relative tunability (up to ~ 40%) and communication quality factor (up to ~ 10 000) under 125 kV/cm.

Keywords: ceramics, thin films, incipient ferroelectric, relaxor behaviour, dielectric properties

INTRODUCTION

As a consequence of the current trend of miniaturisation of electronic devices, and the challenges for the electronics industry to increase the packing density of components of different materials, the miniaturisation process has become a crucial aspect of research in the area of materials engineering [1, 2, 3]. After semiconductors, functional insulators have been gradually included in the miniaturisation process, including ferroelectric materials [4]. Due to their particular properties, ferroelectrics are attractive for a wide range of applications. Their high dielectric response is being used in capacitor applications, their piezoelectric properties utilised in transducers, pyroelectricity in sensors, nonlinear effects in electro-optic devices and their ferroelectric behaviour (polarisation switching) is being attractive for memory applications.

In the field of ferroelectrics miniaturisation, high permittivity strontium titanate (SrTiO_3 , STO) and STO-based materials in a thin layer form have been investigated. In particular, the high tunability of their dielectric permittivity by an electric field has been used in radar and communication applications, including military, airport and police radars, satellite communication systems, mobile phones and wireless computer networks [5, 6]. Currently, the use of Ba-doped STO in tunable microwave devices is under consideration for industrial applications due to the substantial cost

reduction, comparing with single crystals [7]. However, Bi doping is also known to induce a polar state in STO, and thus can be considered for tunable device applications as well [8-23].

The influence of Bi doping on the dielectric properties of STO was first found by Skanavi et al. and explained using an “ionic hopping” model [8]. However, later studies pointed to ferroelectric behaviour with a diffuse phase transition for this system [9]. Indeed, more recent systematic studies of $\text{Sr}_{1-1.5x}\text{Bi}_x\text{TiO}_3$ ceramics clearly demonstrated the dependency of the dielectric response on the Bi concentration, with a crossover from the ferroelectric to a relaxor type behaviour [10-23]. However, the influence of Bi on the structural, microstructural and dielectric properties of STO films has been much less investigated [24-28], and has not been studied and reported systematically.

STATE OF THE ART

Strontium Titanate

SrTiO_3 falls into the unique category of ferroelectrics known as incipient ferroelectrics (or quantum paraelectrics) [29], along with KTaO_3 , CaTiO_3 and TiO_2 [30]. STO has a high real part of dielectric permittivity ϵ' that follows the Curie-Weiss law in the paraelectric regime, but saturates at cryogenic temperatures rather than exhibiting the expected ferroelectric discontinuity [29, 30], being thus described by the Barrett relation derived from the mean-field theory including quantum fluctuations [31].

The imaginary part of the dielectric permittivity ϵ'' of STO is much smaller, typically by a factor of 10^3 , when compared to ϵ' [32]. With decreasing temperature ϵ'' increases steadily, however, with two characteristic loss peaks in the vicinity of 10 K and 80 K. At these temperatures, ϵ'' reveals dispersion effects characteristic of the dielectric relaxation phenomena. The 10 K peak was attributed to an unknown impurity or defect [33, 34]. The 80 K peak was explained in terms of the

dynamics of the elastic domain walls [35] and was not observed for STO single crystals in single-domain state [33].

The dielectric response of thin films reflects the effects of an interfacial “dead layer” between film and electrode, the strain/stress influence of substrates, the presence of grain boundaries (for polycrystalline films), defects (cracks, porosity), etc. [36-40]. As a result, the magnitude and behaviour of the dielectric properties of STO films are strongly dependent on the film’s fabrication method (the type of deposition, parameters of the process), thickness of the film, type of substrates, electrode materials, configuration of capacitors (planar or parallel-plate geometry), etc. In general, the dielectric response of STO films is lower than that reported for their bulk counterpart (either single crystals or ceramics). An illustration of this behaviour is presented in Figure 1, in which the typical temperature dependence of the real part of dielectric permittivity ϵ' of STO is plotted for single crystals, ceramics and films [29, 41, 42].

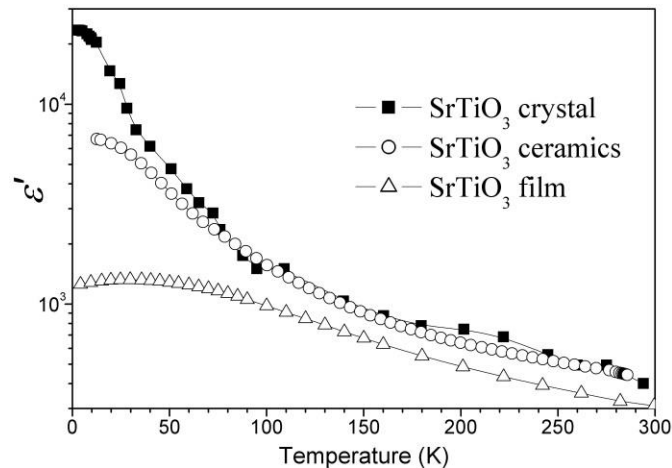


Figure 1. Temperature dependence of the real part of dielectric permittivity ϵ' of: SrTiO₃ single crystal (solid squares) measured along [110] direction, sol-gel derived ceramics (open circles) and pulsed laser deposited 800-nm-thick film (open triangles) measured in parallel-plate-capacitor geometry (adapted from Refs. [29,41,42]), revealing a marked decrease of the permittivity of STO films, when compared with ceramics and single crystals and an appearance of a broad peak in the low-temperature regime.

It is important to stress from Figure 1 that, in contrast to STO single crystals (and ceramics), in which ϵ' saturates below 10 K, a broad peak could be detected in STO thin films at about 30 K. Such a broad peak in ϵ' was observed in many STO films, deposited by different methods and on different substrates, and is usually attributed to the appearance of ferroelectricity [43-46]. In contrast to ϵ' , for which the maximum value is usually at least one order of magnitude smaller for STO films compared to STO crystals, the $\tan \delta$ of STO thin films ($\sim 10^{-2}$) is usually about 10 times higher than that of single crystals ($\sim 10^{-3}$) in all temperature ranges [47]. Meanwhile, similar to ceramics, the properties of STO films can be also modified by doping with different chemical elements, or by preparation method.

Sr_{1-1.5x}Bi_xTiO₃ Ceramics

The incorporation of dopant ions into the STO lattice depends on the ionic size and electronic structure of both dopant and host ions. In the case of STO, the host ions are Sr²⁺ and Ti⁴⁺ with sizes of 1.44 Å and 0.605 Å, respectively [48]. Since the perovskite structure of strontium titanate with a general formula ABO₃ is very closely packed, there are two kinds of possible substitution: at the Sr²⁺ site (or A-site) and at the Ti⁴⁺ site (or B-site). However, from the reported results, it appears that isovalent B-site dopants, such as Zr⁴⁺, Sn⁴⁺, Ge⁴⁺, Mn⁴⁺, have a much smaller effect on dielectric properties of STO, compared to isovalent A-site dopants [49, 50], namely Ca²⁺ [51-54], Ba²⁺ [55, 56], Pb²⁺ [57], Cd²⁺ [58], Mn²⁺ [59-63] as well as trivalent rare-earth ions La³⁺, Pr³⁺, Nd³⁺, Sm³⁺, Gd³⁺, Tb³⁺, Dy³⁺, Ho³⁺, Er³⁺, Tm³⁺, Yb³⁺, Lu³⁺ [64-68], and Y³⁺ [69, 70].

The dielectric properties of the Sr_{1-1.5x}Bi_xTiO₃ (SBiT) system were first investigated in ceramics by Skanavi et al. in 1957 [8]. In this study, a high peak in the temperature dependence of the real part of dielectric permittivity $\epsilon'(T)$ with frequency dispersion, induced by moderate Bi dopant concentrations in STO was reported. The authors suggested a polarisation mechanism by “hopping ions”, rather than the occurrence of ferroelectricity.

However, based on the observation of the slim hysteresis loop in Bi-doped STO, Smolenskii et al. suggested a ferroelectric mechanism with the so called “diffuse phase transition” [9, 71]. Later several researchers systematically studied Bi-doped STO system, establishing the relations between the structural and the dielectric response of Bi-doped STO ceramics [10-23, 72, 73].

In contrast to Ba-, Pb- and Ca-doped STO systems, $\text{Sr}_{1-1.5x}\text{Bi}_x\text{TiO}_3$ is a solid solution, in which the host Sr^{2+} ions are substituted by heterovalent Bi^{3+} ions. Thus, to satisfy the charge neutrality, a strontium vacancy V_{Sr} has to be created upon the substitution of three divalent Sr^{2+} ions by two trivalent Bi^{3+} ions. Hence the appropriated chemical formula $[\text{Sr}_{1-1.5x}(\text{V}_{\text{Sr}})_{0.5x}\text{Bi}_x]\text{TiO}_3$ should be considered. Therefore, the solid solubility of Bi in the STO lattice is restricted up to $x = 0.20$ [10, 12]. Below this solid solubility limit, room-temperature X-ray diffraction profiles exhibit a cubic structure for Bi-doped STO.

Detailed studies of the dielectric properties of $\text{Sr}_{1-1.5x}\text{Bi}_x\text{TiO}_3$ ceramics over wide temperature (Figures 2, 3 and 4) [21] and frequency [72] ranges revealed a complex structure of the dielectric response. Several relaxation processes were observed. Moreover, for some concentration of Bi, $\text{Sr}_{1-1.5x}\text{Bi}_x\text{TiO}_3$ ceramics were referred to as relaxor [10, 12]. The main typical characteristics for relaxor behaviour are following [74, 75, 76]:

- rounded peaks occur in the temperature dependence of ε' , in contrast to the sharp peak at the phase transition temperature observed for the classic ferroelectrics;
- temperature of the ε' peak is always higher than the temperature of the loss peak;
- temperature dependence of the ε' obeys the relation: $1/\varepsilon' - 1/\varepsilon'_{\text{max}} = (T - T_{\text{max}})^\gamma / C$, with exponent γ close to 2, but not to 1 as for the classic ferroelectrics with $\varepsilon'(T)$ following the Curie-Weiss law;
- the maximum ε' decreases in value, and its temperature shifts to higher temperatures with increasing measurement frequency, while the properties of classic ferroelectrics do not vary intensely with frequency in the radio frequency range:

- a square-to-slim transition of the hysteresis loops with the remanent polarisation decreasing with increasing temperature and tailing off to zero in the diffuse range, in contrast to a sharp decrease to zero in classic ferroelectrics;
- a compliance with a Vögel-Fulcher relation, etc.

Thus, for $\text{Sr}_{1-1.5x}\text{Bi}_x\text{TiO}_3$ ceramics, three concentration regions with different dielectric properties were identified [21].

1. $\text{Sr}_{1-1.5x}\text{Bi}_x\text{TiO}_3$ ceramics with low Bi concentration ($x = 0.0005-0.002$). Two dielectric anomalies at ~ 18 and ~ 30 K at ~ 100 Hz (denoted as modes *A* and *B*, respectively, in Figure 2) are induced on the quantum paraelectric background of STO. These anomalies are frequency dependent, but the temperature (T_{max}) where the dielectric permittivity maximum occurs is independent of Bi concentration.
2. $\text{Sr}_{1-1.5x}\text{Bi}_x\text{TiO}_3$ ceramics with intermediate Bi concentration ($x = 0.0033 - 0.0267$). When Bi concentration $x > 0.0033$, an additional peak (mode *C*) appears in ϵ' (Figure 3 left picture) and ϵ'' (Figure 3 right picture). It should be emphasised that the T_{max} of mode *C* increases with increasing Bi concentration, which can be seen more clearly in ϵ'' (Figure 3 right picture). This is similar to the behaviour of typical ferroelectric solid solutions, but different from that of modes *A* and *B*. In the Bi concentration range of $0.0033 < x < 0.0267$, the coexistence of peaks *A*, *B*, and *C* is an interesting characteristic of Bi-doped STO.
3. $\text{Sr}_{1-1.5x}\text{Bi}_x\text{TiO}_3$ ceramics with high Bi concentration ($x = 0.04 - 0.2$). Further increasing Bi concentration to $x > 0.04$, mode *C* predominates, as shown in Figure 4.

In a dielectric material, if the dielectric relaxation process is governed by a thermally activated motion, the temperature dependence of the relaxation time follows the Arrhenius law [77]:

$$\tau = \tau_0 \times \exp[E_a/k_B T] \quad (1)$$

where τ_0 is the preexponential term, E_a is the activation energy, k_B stands for Boltzmann's constant and T is temperature.

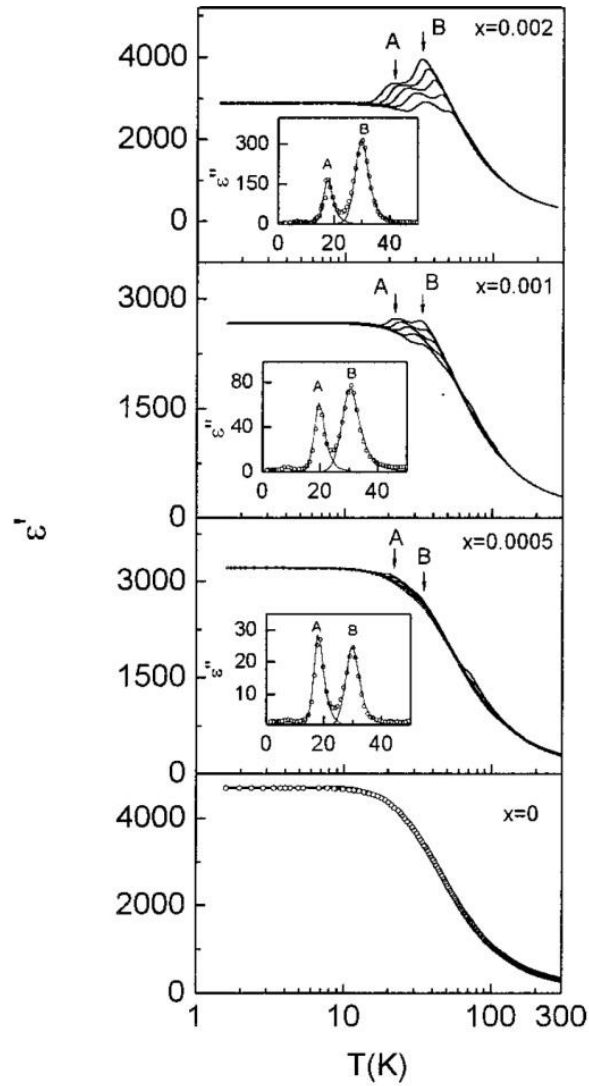


Figure 2. Temperature dependences: of ϵ' for $\text{Sr}_{1-1.5x}\text{Bi}_x\text{TiO}_3$ ceramics with $x = 0, 0.0005, 0.001$ and 0.002 at 0.1, 1, 10, 100 and 1000 kHz (from top to bottom). The inset shows the temperature dependence of ϵ'' at 0.1 kHz. (Reproduced from [Ang, C., Yu, Z. 2002. *J. Appl. Phys.* 91:1487-1494], with the permission of AIP Publishing).

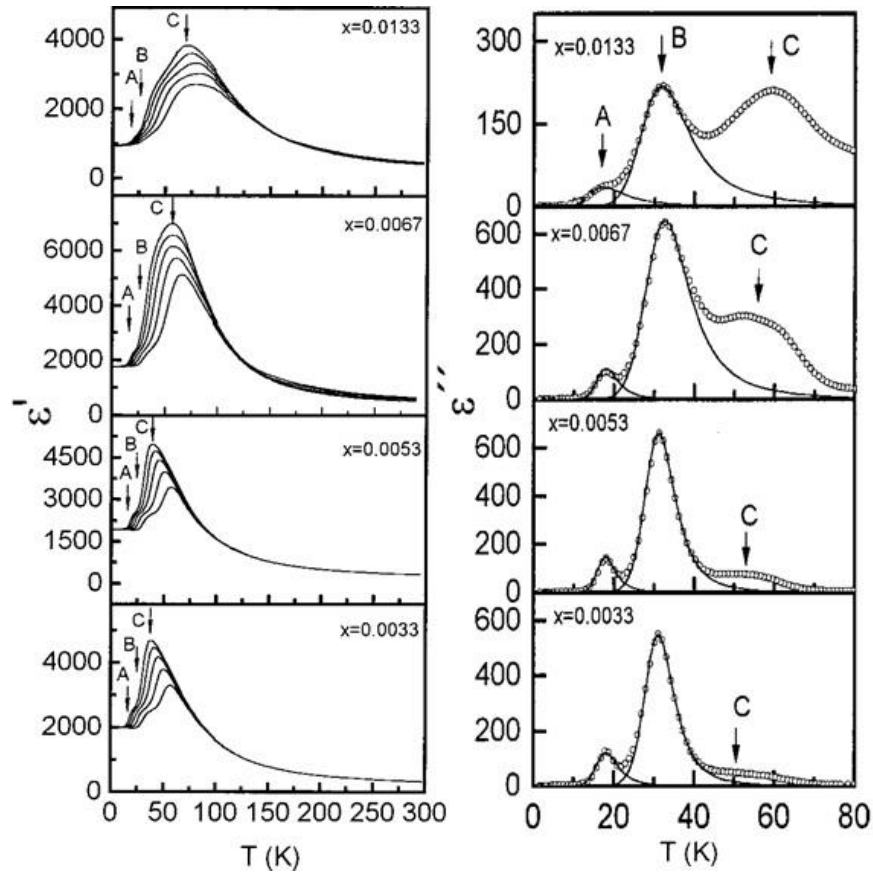


Figure 3. Temperature dependences: of ϵ' at 0.1, 1, 10, 100 and 1000 kHz (from top to bottom) (left picture) and ϵ'' at 0.1 kHz (right picture) for $\text{Sr}_{1-1.5x}\text{Bi}_x\text{TiO}_3$ ceramics with $x = 0.0033, 0.0053, 0.0067$ and 0.0133 . (Reproduced from [Ang, C., Yu, Z. 2002. *J. Appl. Phys.* 91:1487-1494], with the permission of AIP Publishing).

It is found that the relaxation times of modes A and B follow the Arrhenius law in the frequency window of $10 - 10^9$ Hz [21]. For all Bi-doped STO ceramics the results show that, 1) the mean relaxation rates for modes A and B strictly follow the Arrhenius law behaviour in the experimentally accessible frequency domain; 2) the energy barrier $E_a = 62 \pm 2$ meV and the preexponential term $\tau_0 = \sim (0.4 - 1) \times 10^{-13}$ s for mode B, and $E_a = 33 \pm 1$ meV, and $\tau_0 = \sim (0.4 - 2) \times 10^{-13}$ s for mode A, for the samples with $0.0005 \leq x \leq 0.0267$.

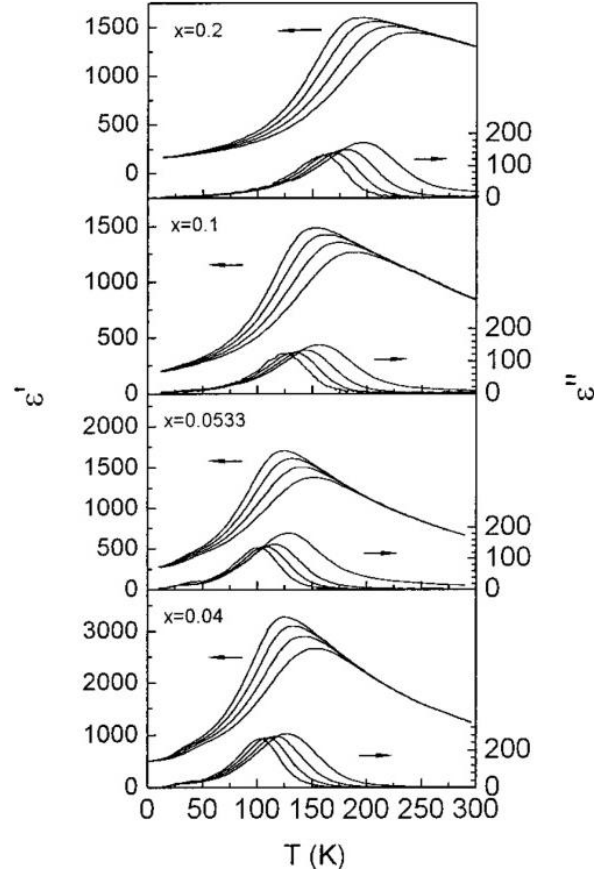


Figure 4. Temperature dependences: of ϵ' and ϵ'' for $\text{Sr}_{1-1.5x}\text{Bi}_x\text{TiO}_3$ ceramics with $x = 0.04, 0.053, 0.1$ and 0.2 at $0.1, 1, 10$ and 100 kHz (ϵ' : from top to bottom, and ϵ'' : from left to right). (Reproduced from [Ang, C., Yu, Z. 2002. *J. Appl. Phys.* 91:1487-1494], with the permission of AIP Publishing).

It was shown that the temperature dependence of the relaxation time for mode C can be well fitted to the Vögel-Fulcher relation:

$$\tau = \tau_0 \times \exp\left[\frac{E_a}{k_B(T_{max} - T_F)}\right] \quad (2)$$

where T_{max} stands for the temperature of the ϵ' maximum and T_F is the static freezing temperature at which the relaxation time τ tends to infinity [78]. $E_a = 36$ meV, $T_F = 30.7$ K, and $\tau_0 = 1 \times 10^{-10}$ s for the sample with $x = 0.0133$

and $E_a = 40$ meV, $T_F = 70.3$ K and $\tau_0 = 5.78 \times 10^{-10}$ s for $x = 0.0533$ were obtained [21].

It was also reported that for $\text{Sr}_{1-1.5x}\text{Bi}_x\text{TiO}_3$ with $x = 0.002$ the amplitudes of *A* and *B* modes in ϵ' gradually decrease under a *dc* electric field up to 35 kV/cm, but their T_{max} values are not shifted that is also valid for the temperatures of the ϵ'' maxima [21]. The latter fact provides evidence that modes *A* and *B* are different from the relaxor mode, whose T_{max} values are electric-field dependent. At higher fields, a broad ϵ' peak, similar to that observed in undoped STO under *dc* bias, is induced, although the temperature range of the field dependent ϵ' is expanded, from about 0 - 80 K for undoped STO, to about 0 - 150 K for Bi-doped STO.

Moreover, the remanent polarisation P_r , obtained from the hysteresis loops of Bi-doped STO ceramics with the concentration range of $x = 0.0133$ - 0.2, first increases with rising temperature until a maximum at about 80 K, and then decreases with further temperature increase. However, it does not disappear at T_{max} , but inflects and tails off to zero, as in typical relaxors. Therefore, this relaxation process was assigned as relaxor-type behaviour, originated from off-centre Bi dipoles, forming dipole clusters due to the local inhomogeneous distribution of Bi^{3+} ions [21].

It was concluded that Sr-site vacancies are induced in Bi-doped STO due to the charge imbalance. Thus, two local environments in the STO lattice can be considered for Bi ions: *i*) Bi ions without any Sr vacancy nearby and *ii*) Bi ions with a Sr vacancy nearby (schematic illustration in [21]). Meanwhile, Bi^{3+} ions at the Sr sites are supposed to have off-centre displacement, which leads to the formation of dipoles. Therefore, the occurrence of the two dielectric modes *A* and *B* was proposed to arise from the different ionic displacements for two types of dipoles: off-centre Bi ions with a neighbouring Sr vacancy and those without it [21].

Thus, the dielectric behaviour of $\text{Sr}_{1-1.5x}\text{Bi}_x\text{TiO}_3$ is characterised by a broadened ϵ' peak with the temperature of ϵ' maximum shifted to higher temperatures as the frequency increases that is generally called relaxor behaviour. Moreover, two types of polar dielectric relaxation were introduced by Bi^{3+} ions in STO ceramics: 1) modes *A* and *B* occurring at low Bi concentrations described by Arrhenius law and related to individual off-

centre Bi^{3+} ions on Sr sites with and without Sr vacancies nearby and 2) mode C following the Vögel–Fulcher relation and attributed to polar clusters formed by interacting $\text{Bi}^{3+}_{\text{Sr}}$ dipoles at higher Bi content [21].

In spite of all this knowledge on STO single crystals and ceramics (doped and non-doped) the understanding of STO films electrical behaviour and its dependence on dopants is much less comprehensive. In the next section, an overview of the work conducted by the authors on structural, microstructural and electric characterisation of polycrystalline $\text{Sr}_{1-1.5x}\text{Bi}_x\text{TiO}_3$ thin films will be presented. The dielectric behaviour of the films, studied over wide frequency, electric field and temperature ranges, will be compared with that of equivalent ceramics. The reasoning for the observed differences is hypothesised and discussed.

METHODS

Preparation

$\text{Sr}_{1-1.5x}\text{Bi}_x\text{TiO}_3$ (SBiT) thin films with $x = 0, 0.0053, 0.04, 0.1, 0.167$ and 0.267 were prepared by sol-gel method and studied. For the preparation of the sols with a concentration of about 0.2 M, the following reagents were used in proportions depending on the film's composition: strontium acetate $\text{C}_4\text{H}_6\text{O}_4\text{Sr}$ (98%, ABCR), tetra-n-butyl orthotitanate $\text{C}_{16}\text{H}_{36}\text{O}_4\text{Ti}$ (98%, MERCK), bismuth acetate $\text{C}_6\text{H}_9\text{BiO}_6$ (99%, ABCR), acetic acid $\text{C}_2\text{H}_4\text{O}_2$ (99.8%, MERCK), 1,2-propanediol $\text{C}_3\text{H}_8\text{O}_2$ (99.5%, Riedel-de Haën) and absolute ethanol $\text{C}_2\text{H}_6\text{O}$ (99.8%, MERCK).

Using the previously prepared precursor solutions, layers were deposited on the substrates by spin-coating at 4000 rpm for 30 s. Before utilisation, the substrates were cleaned in boiling ethanol and dried on a hot plate. Subsequently, the films (substrate with wet layer) were heated on a hot plate at 350°C for ~ 1 min. This step was repeated after each spinning to ensure complete removal of volatile species between each layer. After the deposition of the required number of layers (in this work it is equal to 10

layers), they were annealed in air at 750°C for 60 min. All Bi-doped STO films were deposited on Si/SiO₂/TiO₂/Pt substrates (Inostek Inc., Korea).

Characterisation

The influence of the incorporation of Bi ions into the Sr sites of STO films on the structure and microstructure was studied, using X-ray diffraction (XRD, Rigaku D/Max-B, Cu K α), scanning electron microscopy (SEM, Hitachi S-4100) and scanning probe microscopy (SPM, Multimode, Nanoscope IIIA, Digital Instruments). Dielectric measurements were carried out in parallel plate capacitor geometry for single-phase polycrystalline Bi-doped STO films on Si/SiO₂/TiO₂/Pt substrates with Au as top and Pt as bottom electrodes. Dielectric response was measured in the frequency range of 100 Hz - 1 MHz, temperature range of 10-300 K and *dc* electric field range of 0-125 kV/cm, and completed by polarisation *vs* electric field measurements at 100 Hz from 10 to 300 K, using a Precision LCR Meter (HP 4284A) and a ferroelectric tester (TF analyser 1000 AIXACT), respectively, in a He closed cycle cryogenic system (Displex ADP-Cryostat HC-2) controlled by a digital temperature controller with silicon diode thermometers (Scientific Instruments model 9650).

RESULTS

Crystal Structure

The XRD patterns of Sr_{1-1.5x}Bi_xTiO₃ (SBit) thin films with $x = 0, 0.0053, 0.04, 0.167$ and 0.267 deposited on Si/SiO₂/TiO₂/Pt substrates and annealed at 750°C are depicted in Figure 5.

Besides the diffraction peaks of the substrate, only reflections of the cubic STO system are observed for all the samples with concentrations of Bi $x \leq 0.167$, whereas the second phase Bi₄Ti₃O₁₂ is detected for the doping concentration $x = 0.267$. These results are in accordance with Sr_{1-1.5x}Bi_xTiO₃

ceramics, in which the single phase compositions were obtained for $x \leq 0.20$ and $\text{Sr}_2\text{Bi}_4\text{Ti}_5\text{O}_{18}$, $\text{Bi}_4(\text{TiO}_4)_3$ and $\text{Bi}_2\text{Ti}_4\text{O}_{11}$ second phases were identified for ceramics samples with $0.227 \leq x \leq 0.267$ [22].

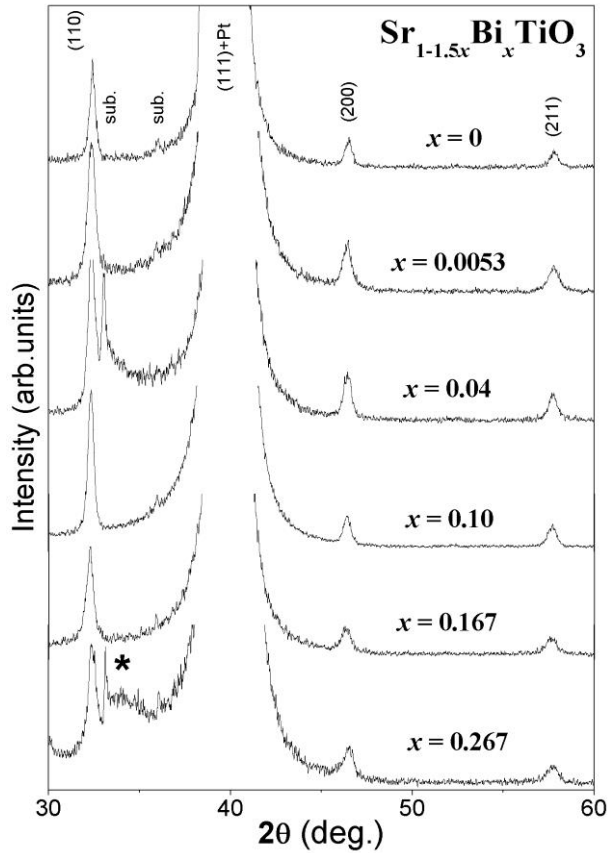


Figure 5. X-ray diffraction patterns of $\text{Sr}_{1-1.5x}\text{Bi}_x\text{TiO}_3$ thin films, * denotes $\text{Bi}_4\text{Ti}_3\text{O}_{12}$ second phase, *sub.* denotes substrate peaks, *Pt* denotes peak of Pt layer, while STO peaks are marked by corresponding indexes.

The lattice parameter c of SBIT films, deduced from the XRD patterns as shown in Figure 6, increases with increasing Bi content from $\sim 3.905 \text{ \AA}$ for undoped STO to $\sim 3.913 \text{ \AA}$ for $x = 0.167$, with a slope of about 0.038 \AA .

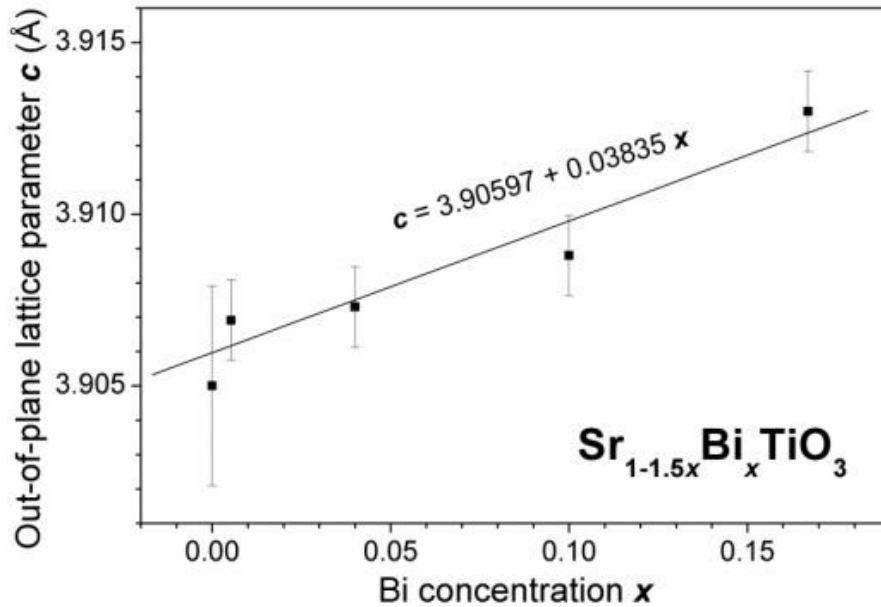


Figure 6. Lattice parameter c of $\text{Sr}_{1-1.5x}\text{Bi}_x\text{TiO}_3$ films as a function of Bi concentration.

A similar increase of the lattice parameter was reported for SBiT ceramics as well [10, 22], but it was not explained, probably because Bi^{3+} ions with coordination numbers of 6 and 8 are much smaller than Sr^{2+} ions while there is no data for Bi^{3+} with the coordination number of 12 [48]. However, linear extrapolation of the ionic radius values of $\text{Bi}_{(5)}^{3+}$, $\text{Bi}_{(6)}^{3+}$ and $\text{Bi}_{(8)}^{3+}$ to the coordination number of 12, as shown in Figure 7, reveals that the predicted ionic radius of $\text{Bi}_{(12)}^{3+}$ is 1.45 Å, i.e., it is slightly larger than the substituted Sr^{2+} ions (ionic radius of $\text{Sr}_{(12)}^{2+} = 1.44$ Å). Therefore, an increase of the lattice parameter in $\text{Sr}_{1-1.5x}\text{Bi}_x\text{TiO}_3$ films and ceramics with increasing Bi content can be expected [79]. Moreover, the assumption that the expansion of the unit cell is also due to the formation of V_{Sr} , and a corresponding electrostatic repulsion of adjacent oxygen anions, can be considered to be reasonable as well [80].

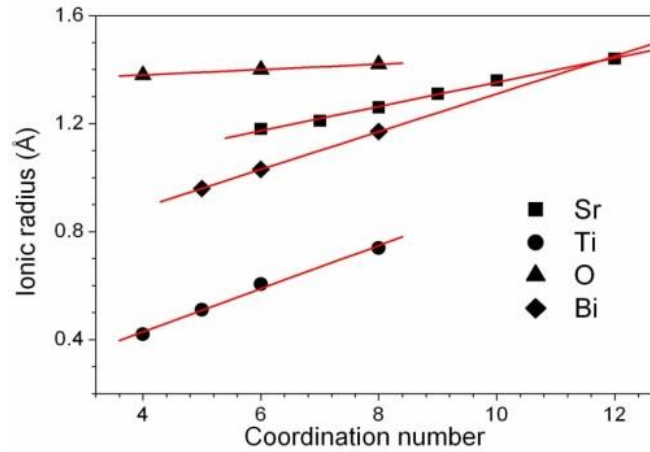


Figure 7. Linear variations of ionic radii of several ions *versus* coordination number following [48], including extrapolation to a coordination number of 12 for Bi^{3+} ions.

Microstructural Analysis

The microstructure of $\text{Sr}_{1-1.5x}\text{Bi}_x\text{TiO}_3$ films deposited on $\text{Si}/\text{SiO}_2/\text{TiO}_2/\text{Pt}$ substrates was analysed by SEM and SPM at room temperature. SEM cross-section micrographs of $\text{Sr}_{1-1.5x}\text{Bi}_x\text{TiO}_3$ films with $x = 0, 0.0053, 0.04$ and 0.167 are shown in Figure 8. It is seen that SBiT films exhibit a crack-free, continuous and fine-grained microstructure without particulates (Figure 8). The thickness of the studied films was estimated to be ~ 450 nm, independent of Bi concentration.

The surface morphology of $\text{Sr}_{1-1.5x}\text{Bi}_x\text{TiO}_3$ films with $x = 0, 0.053, 0.04$ and 0.167 analysed by SPM at room temperature are depicted in Figure 9, as in-plane surface and 3D view (*inset*) micrographs of SBiT thin films. Confirming the results obtained from the SEM study, all SBiT films show a smooth surface with a roughness of 1 - 2 nm and an average grain size of $\sim 80 - 120$ nm. 3D images of SBiT films revealed that the grains were grown in all three x, y, z -directions. The SPM derived average in-plane grain size and roughness of undoped and Bi-doped STO films are plotted in Figure 10 as a function of the Bi content.

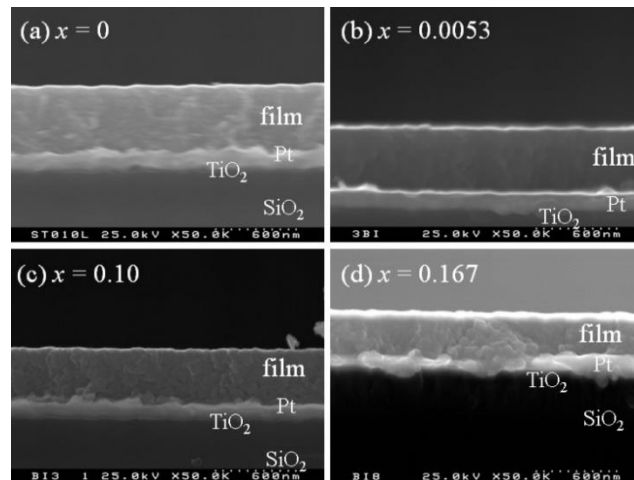


Figure 8. SEM cross-section micrographs of $\text{Sr}_{1-1.5x}\text{Bi}_x\text{TiO}_3$ thin films with $x = 0$ (a), 0.0053 (b), 0.04 (c) and 0.167 (d).

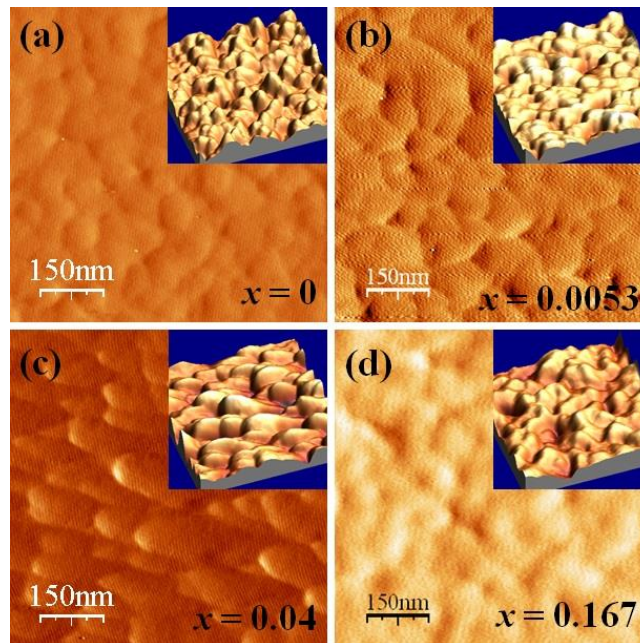


Figure 9. SPM micrographs of $\text{Sr}_{1-1.5x}\text{Bi}_x\text{TiO}_3$ films with $x = 0$ (a), 0.0053 (b), 0.04 (c) and 0.167 (d).

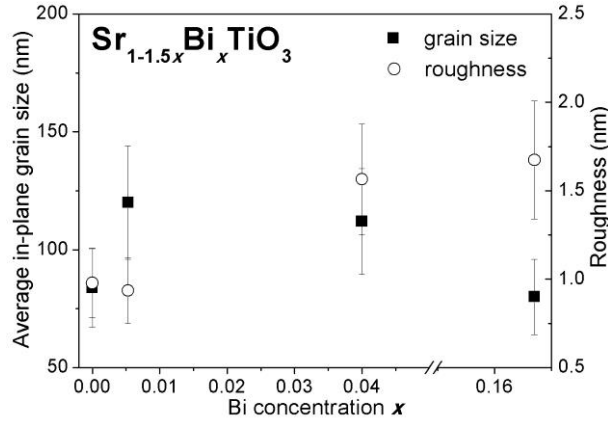


Figure 10. Average grain size (solid squares, *left axis*) and roughness (open circles, *right axis*) versus Bi concentration of $\text{Sr}_{1-1.5x}\text{Bi}_x\text{TiO}_3$ films.

Compared to undoped STO films, a small Bi doping content increases the grain size. However, the variation of the grain size with the Bi concentration is not monotonous; after an initial increase, the grain size decreases with further increase of the dopant content (Figure 10 *left axis*). The roughness of all the studied samples slightly increases with the dopant content (Figure 10 *right axis*). As was reported in the literature, no systematic variation of the grain size with a change in the Bi concentration was observed as well in $\text{Sr}_{1-1.5x}\text{Bi}_x\text{TiO}_3$ ceramics [22].

Low Temperature Dielectric Properties as a Function of Frequency

Temperature dependence of the real part of the dielectric permittivity ϵ' of $\text{Sr}_{1-1.5x}\text{Bi}_x\text{TiO}_3$ films with $x = 0, 0.0053, 0.04, 0.10, 0.167$ at 4 kHz is depicted in Figure 11. The magnitude of the peak (ϵ'_{max}) depends on Bi content, and the temperature of ϵ'_{max} (T_{max}) increases with Bi concentration, as plotted in Figure 12. A marked increase from ~ 270 to ~ 370 is observed in ϵ'_{max} for low dopant concentrations, varying from $x = 0$ to $x = 0.0053$, being followed by a non-monotonous variation for higher Bi content. The highest $\epsilon'_{max} \sim 500$ is observed for $x = 0.04$. The increase of ϵ'_{max} for small x ,

and a later decrease for high x , was also observed in SBiT ceramics, where the increase in Bi concentration leads to a variation of ϵ'_{max} and a shift of T_{max} to higher temperatures [10, 12]. The highest value of ϵ'_{max} in $\text{Sr}_{1-1.5x}\text{Bi}_x\text{TiO}_3$ ceramics was observed at $x = 0.0067$ ($\epsilon'_{max} \sim 6000$ at $T_{max} \sim 66$ K) [12]. Moreover, in contrast to the SBiT films analysed here, two induced anomalies occurred in $\epsilon'(T)$ of $\text{Sr}_{1-1.5x}\text{Bi}_x\text{TiO}_3$ ceramics: at ~ 18 K and at ~ 30 K (with T_{max} independent of x), whereas one more dielectric anomaly (whose T_{max} increases with increasing Bi content) was observed for $x \geq 0.0133$ [17, 21].

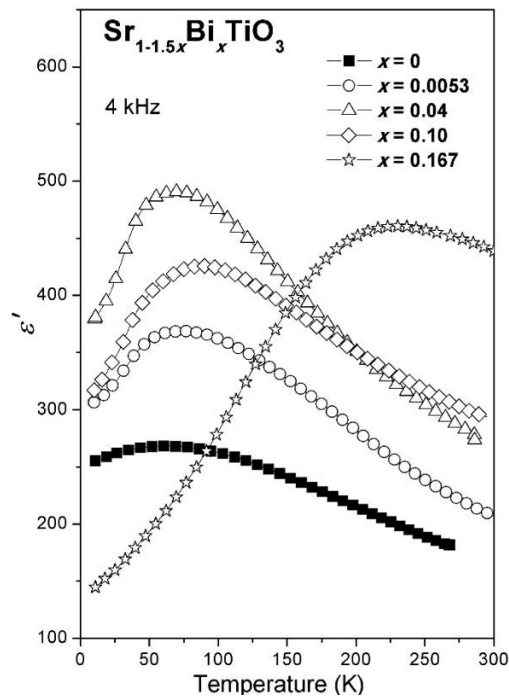


Figure 11. Temperature dependence of the real part of dielectric permittivity ϵ' of $\text{Sr}_{1-1.5x}\text{Bi}_x\text{TiO}_3$ films with $x = 0, 0.0053, 0.04, 0.10, 0.167$ at 4 kHz.

Temperature dependence of imaginary part of the dielectric permittivity ϵ'' and variation of the dissipation factor $\tan\delta = \epsilon''/\epsilon'$ as a function of the temperature of $\text{Sr}_{1-1.5x}\text{Bi}_x\text{TiO}_3$ films with $x = 0, 0.0053, 0.04, 0.10, 0.167$ at 4 kHz are depicted in Figures 13 and 14, respectively. ϵ'' of Bi-doped STO

films is higher than that of undoped STO films. Obtained values of the $\tan\delta$ of SBiT films are higher than those of undoped STO films as well, and increase with increasing Bi content: from $\sim 0.5\%$ for undoped STO films to $\sim 5\%$ for SBiT samples with $x = 0.167$ (Figure 14). Moreover, in contrast to the broad peak at ~ 62 K detected in $\varepsilon'(T)$ of undoped STO films, a strong peak in $\varepsilon'(T)$ of SBiT films (Figure 11), accompanied by strong peaks induced in the losses (Figures 13 and 14), can be easily observed.

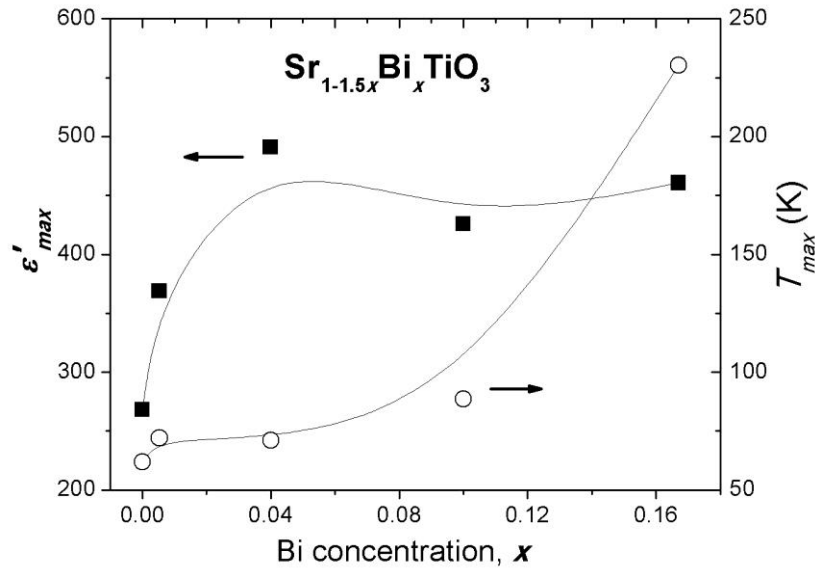


Figure 12. Variation of the maximum of the real part of the dielectric permittivity ε'_{max} (solid squares, *left axis*) and of the temperature of the maximum of the real part of the dielectric permittivity T_{max} (open circles, *right axis*) of $\text{Sr}_{1-1.5x}\text{Bi}_x\text{TiO}_3$ thin films with Bi content at 4 kHz.

The ε'' and $\tan\delta$ of undoped STO films (Figures 13 and 14) were also characterised by three peaks, described as following: 1) peak A could be considered as a stress/strain induced ferroelectric phase transition [43]; 2) peak B was attributed to the dynamics of the elastic domain walls that occur at the cubic-to-tetragonal phase transition around 105 K [35]; 3) peak C observed in some thin films was associated with the effect of defects/impurities such as oxygen vacancies [81, 82].

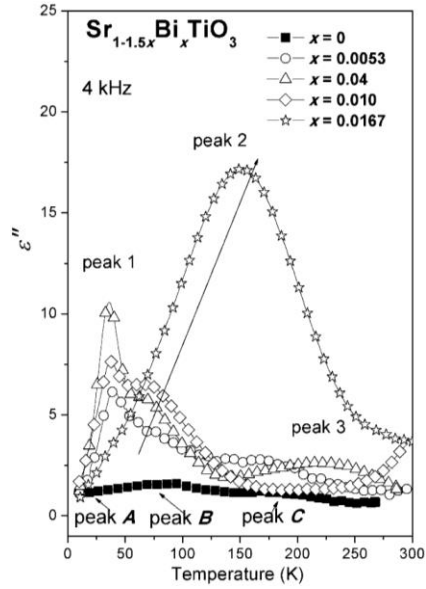


Figure 13. Temperature dependence of the imaginary part of dielectric permittivity ϵ'' of $\text{Sr}_{1-1.5x}\text{Bi}_x\text{TiO}_3$ films with $x = 0, 0.0053, 0.04, 0.10, 0.167$ at 4 kHz.

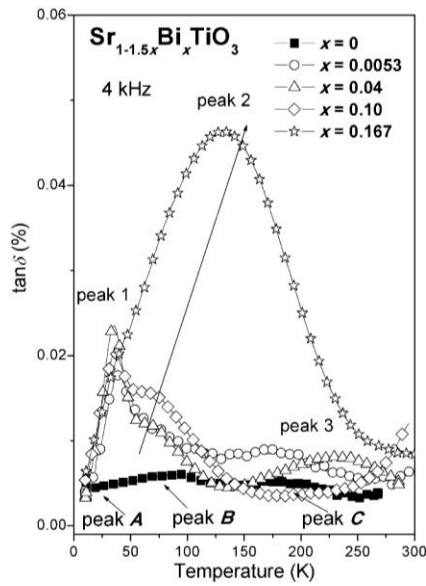


Figure 14. Temperature dependence of the dissipation factor $\tan\delta$ of $\text{Sr}_{1-1.5x}\text{Bi}_x\text{TiO}_3$ films with $x = 0, 0.0053, 0.04, 0.10, 0.167$ at 4 kHz.

For a better understanding of the difference or similarity in nature of peaks 1, 2 and 3 detected in SBiT thin films and peaks A, B and C of undoped STO, a diagram of the temperatures of these peaks, obtained from $\epsilon''(T)$ at 4 kHz, is presented in Figure 15. Peak 1 (almost independent of Bi content) is detectable in $\epsilon''(T)$ of SBiT films with $x \leq 0.10$ at temperatures between 38 K and 56 K. This is much higher than the temperature of peak A in undoped STO films (~ 22 K), implying a difference in the origin of these peaks. Meanwhile, the peak about 30 K was observed in $\epsilon''(T)$ of $\text{Sr}_{1-1.5x}\text{Bi}_x\text{TiO}_3$ ceramics with small Bi concentration ($x \leq 0.04$) [13, 14, 15, 21]. The temperature of this peak in SBiT ceramics was almost independent of the Bi content [13] similar to peak 1 observed in the SBiT films analysed here.

At the same time, peak 2 was detected in SBiT films at different temperatures: from ~ 68 K to ~ 145 K due to strong dependency on Bi content, in contrast to the almost stable peak 1 in the SBiT films, and in contrast to the ~ 85 K at which peak B was detected in the undoped STO films. Thus, the origin of peak 2 in the SBiT films is different from that of peak 1 of the same films, or from that of the peak B of undoped STO films. Similar to peak 2 observed in SBiT films, the relaxor peak appeared in SBiT ceramics, becoming dominant for $x > 0.0267$ [15].

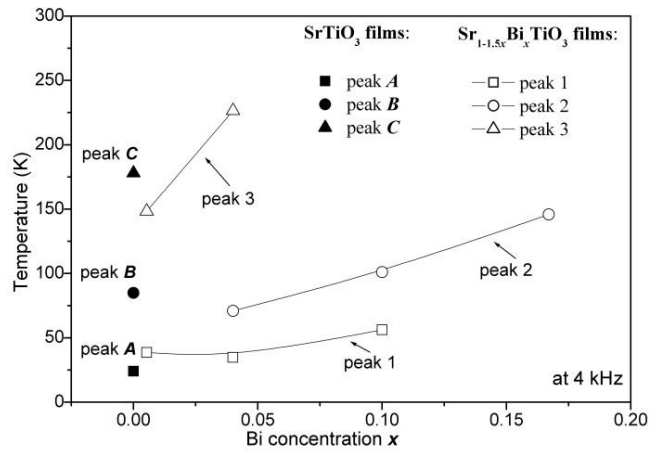


Figure 15. Diagram of temperature positions of peaks 1, 2 and 3 detected in $\text{Sr}_{1-1.5x}\text{Bi}_x\text{TiO}_3$ thin films in comparison to peaks A, B and C of undoped SrTiO_3 obtained from $\epsilon''(T)$ at 4 kHz.

Concerning the very broad, and almost undetectable, peak 3 (not clearly observed at ~ 140 K - ~ 230 K), its position is not far from that of peak C in undoped STO films (~ 180 K). Moreover, as was reported in the literature, similarly broad peak can be observed for undoped STO films at temperatures of ~ 160 - 180 K [81, 82] and for Bi-doped ST ceramics, disappearing after annealing in oxygen or air [18]. Thus, based on this information peak 3 can be associated with oxygen vacancies.

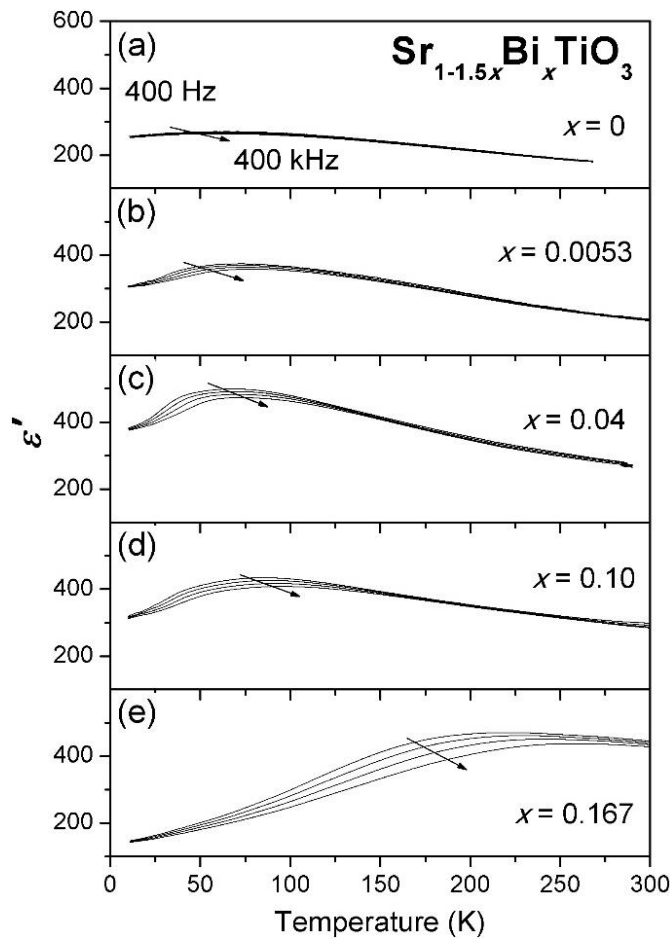


Figure 16. Temperature dependence of real part of dielectric permittivity ϵ' of $\text{Sr}_{1-1.5x}\text{Bi}_x\text{TiO}_3$ films with $x = 0, 0.0053, 0.04, 0.10,$ and 0.167 at 400 Hz, 4 kHz, 40 kHz and 400 kHz.

The analysis of the frequency influence on the real part $\epsilon'(T)$ and imaginary part $\epsilon''(T)$ of the dielectric permittivity, and the examination of the temperature dependence of relaxation times, is helpful in understanding the relaxation mechanism of $\text{Sr}_{1-1.5x}\text{Bi}_x\text{TiO}_3$ films. The frequency dispersion of the dielectric response of SBiT films with $x = 0, 0.0053, 0.04, 0.10$ and 0.167 is shown in Figures 16 and 17, which present $\epsilon'(T)$ at 400 Hz, 4 kHz, 40 kHz and 400 kHz (Figure 16) and $\epsilon''(T)$ at 400 Hz, 4 kHz and 40 kHz (Figure 17).

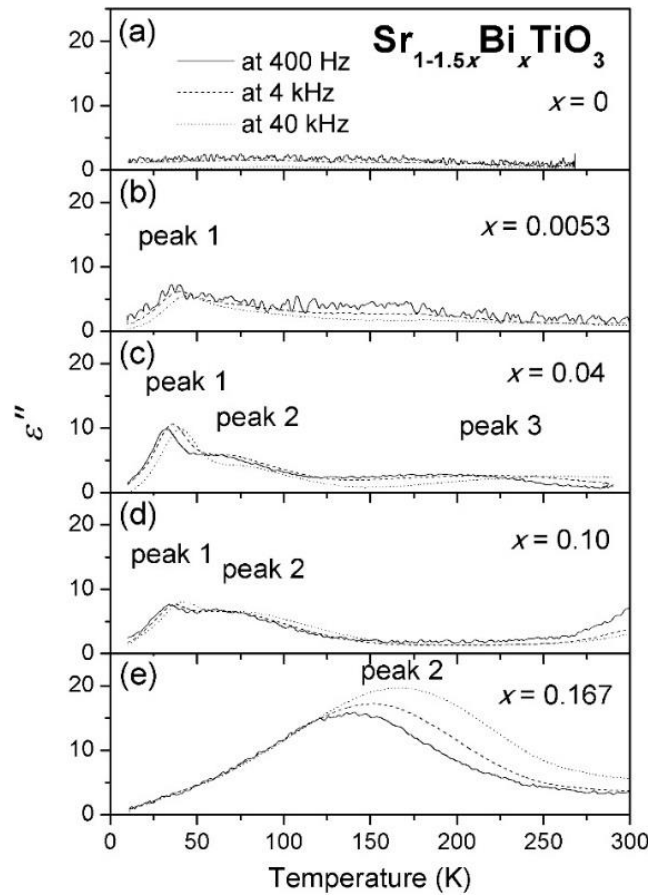


Figure 17. Temperature dependence of imaginary part of dielectric permittivity ϵ'' of $\text{Sr}_{1-1.5x}\text{Bi}_x\text{TiO}_3$ films with $x = 0, 0.0053, 0.04, 0.10, \text{ and } 0.167$ at 400 Hz, 4 kHz and 40 kHz.

A peak is present in all the $\varepsilon'(T)$ curves of the analysed SBiT samples, and at all the measured frequencies (Figure 16). As the frequency increases, the peak becomes broader, ε'_{max} decreases, and the temperature of the maximum T_{max} increases. The shift of T_{max} to higher temperatures, and a suppression of ε'_{max} with frequency increase, becomes more obvious with increasing Bi concentration. Such broadening and frequency dependency of $\varepsilon'(T)$, that becomes more and more visible with increasing Bi content, was also observed in $\text{Sr}_{1-1.5x}\text{Bi}_x\text{TiO}_3$ ceramics [10, 11, 12].

Comparing Figure 17 with Figure 16, one can conclude that T_{max} is always higher than the temperature of the peak in $\varepsilon''(T)$ at equivalent frequency. Moreover, $\varepsilon''(T)$ of SBiT films was also found to be frequency dependent (see Figure 17), and the increase of the peak temperature for the $\varepsilon''(T)$ with measured frequency indicates that the microscopic process of the dielectric anomaly is a thermally activated polar motion.

The Arrhenius law was used for analysis of the Bi induced relaxation processes of SBiT thin films. However, only data points related to peak 1 in $\varepsilon''(T)$ of SBiT thin films with $x \leq 0.10$ are well fitted by straight lines on the Arrhenius plots ($\ln(\tau)$ versus $1000/T_{\varepsilon''_{max}}$). In the case of peak 2, well detectable in the $\varepsilon''(T)$ of SBiT films with $x \geq 0.04$, the pre-exponential term τ_0 appears to be extremely low, and seems to be physically unreasonable. Therefore, the data for such compositions were fitted using an alternative empirical description of relaxation, that is, the Vögel-Fulcher relation. Compared to the Arrhenius law, the empirical Vögel-Fulcher relation includes one additional fitting parameter, T_F , interpreted as a static freezing temperature, at which motion of all dipole moments slows down, and is often used to describe the behaviour of relaxor polar clusters or strongly correlated dipoles in the frequency window of $10^2 - 10^6$ Hz. The fitting parameters of the Arrhenius law (peak 1) and of the Vögel-Fulcher relation (peak 2) for $\varepsilon''(T)$ of Bi-doped STO films are presented in Table 1.

As seen from Table 1, for $\text{Sr}_{1-1.5x}\text{Bi}_x\text{TiO}_3$ films with small Bi content $x \leq 0.10$, the Arrhenius law parameters $E_a = 65-74$ meV and $\tau_0 = (0.4 - 2.5) \times 10^{-14}$ s are obtained for peak 1, detected in $\varepsilon''(T)$ at temperatures as low as ~ 38 K. The Arrhenius law parameters $E_a = 60 - 64$ meV and $\tau_0 = (4 - 10) \times 10^{-14}$ s were obtained in SBiT ceramics as well, for a peak observed about

30 K in $\varepsilon''(T)$ independent of Bi content [21]. By analogy, and due to the similarities in their behaviour, it is possible to assume that peak 1 in SBiT films has an analogous nature to that of the relaxation peak at ~ 30 K observed in SBiT ceramics. Thus, individual polar dipoles formed by off-centre dopant ions, proposed as a relaxation mechanism in SBiT ceramics, can be attributed to peak 1 detected in $\varepsilon''(T)$ of SBiT films with $x \leq 0.10$.

Table 1. Relaxation dynamics parameters of $\text{Sr}_{1-1.5x}\text{Bi}_x\text{TiO}_3$ films, obtained for peak 1 from the fitting to the Arrhenius law, and for peak 2 from the fitting to the Vögel-Fulcher relation

x	Peak 1		Peak 2		
	Arrhenius Law		Vögel-Fulcher Relation		
	E_a (meV)	τ_0 (s)	E_a (meV)	τ_0 (s)	T_F (K)
0.0053	74	1.3×10^{-14}			
0.04	65	2.5×10^{-14}	2	5×10^{-6}	50
0.10	74	0.4×10^{-14}	7	5×10^{-8}	51
0.167			38	4×10^{-9}	102

The relaxation dynamics of the loss peaks in SBiT films with $x = 0.04$ and $x = 0.10$ follows both the Arrhenius law for peak 1 and the Vögel-Fulcher relation for peak 2, with E_a , τ_0 and T_F shown in Table 1. For SBiT films with higher Bi concentration ($x > 0.10$), only peak 2 is well defined in $\varepsilon''(T)$, and only the Vögel-Fulcher relation that describes a polar cluster relaxation can be applied. The switching of relaxation dynamics from Arrhenius law to Vögel-Fulcher relation implies a crossover, from hopping of individual off-centre Bi^{3+} ions to polar clusters reversal, as the dominant mechanism in SBiT films with increasing Bi content, similar to ceramics [21].

As Bi concentration increases, the average distance between Bi dipoles decreases and interaction between the dipoles appears. Therefore, some dipoles form dipole clusters due to the local inhomogeneous distribution of Bi ions, and this leads to the occurrence of peak 2 and its shift to higher temperatures with increasing Bi content. The coexistence of the individual dipoles that contribute to peak 1 and the dipole clusters that contribute to peak 2 is a singular characteristic of Bi-doped STO. With further increases

in Bi concentration (SBiT films with $x > 0.10$), the interaction between the dipoles becomes much stronger, and more dipole clusters are formed. This results in an increase in the intensity of peak 2, and a decrease in the intensities of peak 1 (Figure 18). Finally, at a high Bi doping level, all dipoles form dipole clusters, and only relaxation peak 2 remains. Simultaneously, the freezing temperature T_F increases with Bi content, from $T_F = 50$ K for $x = 0.04$ to $T_F = 102$ K for $x = 0.167$.

For SBiT ceramics with $x = 0.04$, T_F was reported to be about 70 - 74 K [16], which is close to T_F obtained for the equivalent films. Moreover, the increase of T_F with Bi content is observed both in ceramics ($T_F = 91$ K and 112 K for $x = 0.10$ and 0.167, respectively), and films ($T_F = 51$ K and 102 K obtained in current work for SBiT films with $x = 0.10$ and 0.167, respectively), as shown in Table 1. Other parameters of the Vögel-Fulcher relation are found to be similar as well, particularly, $E_a = 38$ meV and $\tau_0 = 5 \times 10^{-9}$ s for SBiT films with $x = 0.167$ are comparable to $E_a = 31 - 39$ meV and $\tau_0 = (2.21 - 5.26) \times 10^{-9}$ s for SBiT ceramics with $x = 0.04 - 0.167$.

Thus, after a low-frequency analysis of the dielectric response of SBiT films, according to the proximity between the relaxation parameters obtained by the Arrhenius law and the Vögel-Fulcher relation for films and ceramic samples, it is possible to summarise that the incorporation of Bi in STO films leads to a similar effect as that observed for SBiT ceramics:

- in SBiT films with low Bi doping ($x < 0.04$), the dynamics of the induced relaxation (peak 1 detected in $\varepsilon''(T)$) were described by the Arrhenius law, similar to SBiT ceramics, and assigned to an individual hopping of the Bi ions;
- with increasing Bi concentration ($0.04 \leq x \leq 0.167$), the interactions between the dipoles or dipole clusters become stronger. It can be considered as a cooperative hopping of the off-centred Bi ions, followed by the highly polarisable host crystal lattice, and corresponds to relaxation peak 2 detected in $\varepsilon''(T)$ of the analysed SBiT films, with dynamics described by the Vögel-Fulcher relation.

On the other hand, the observation of only one peak independent of Bi content in the $\varepsilon''(T)$ of SBiT films, compared to two peaks, detected at low temperatures in the $\varepsilon''(T)$ of corresponding SBiT ceramics can be first of all related to the much lower grain size of the films and thereby higher tolerance to the lattice defects, including Sr vacancies. In addition, substrate induces strain/stress states that are not present in bulk ceramics. Moreover, the high degree of homogeneity of the studied sol-gel derived films (higher than that in conventionally prepared ceramics) can prevent the segregation of Bi ions, suppressing the interaction between the dipoles created by the off-centre Bi ions for SBiT films with low Bi concentration. Therefore, the peak 2 observed in SBiT films has lower intensity than that in corresponding ceramics.

***P(E)* Hysteresis Response**

The polar nature of the dielectric anomaly observed in $\text{Sr}_{1-1.5x}\text{Bi}_x\text{TiO}_3$ films with $x = 0, 0.04$ and 0.10 was further studied by the measurement of the $P(E)$ curves, shown in Figures 18, 19 and 20, respectively. Hysteresis response of SBiT films was measured at 100 Hz under applied *ac* voltage up to ~ 5 V at different temperatures.

S-shaped loops were observed in the analysed SBiT films with $x = 0.04$ (Figure 19) in comparison to undoped STO (Figure 18). The highest remanent polarisation and coercive field are $P_r = \sim 0.40 \mu\text{C}/\text{cm}^2$ and $E_c = \sim 12.7 \text{ kV}/\text{cm}$ at 15 K (Figure 19a), decreasing with increasing temperature (Figure 19b-f).

Figure 20 depicts the $P(E)$ hysteresis loops of SBiT films with $x = 0.10$. In contrast to the previous SBiT films, the loops are very slim, without a well-defined *S*-shape. P_r and E_c values also decrease, from $P_r = \sim 0.20 \mu\text{C}/\text{cm}^2$ and $E_c = \sim 6.1 \text{ kV}/\text{cm}$ at 15 K toward zero at room temperature.

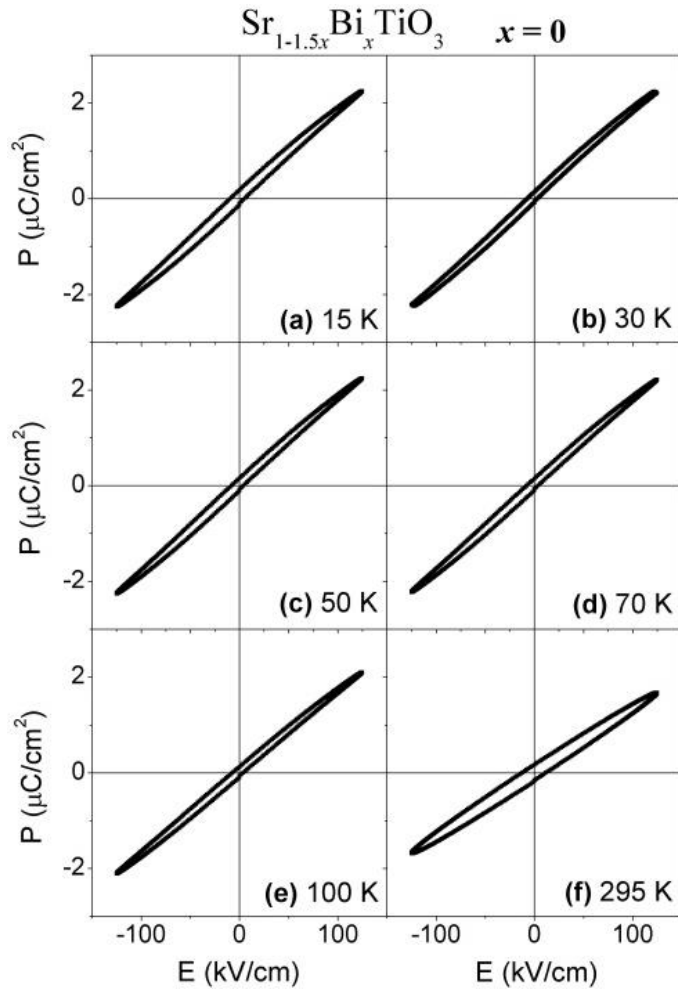


Figure 18. $P(E)$ hysteresis loops of $\text{Sr}_{1-1.5x}\text{Bi}_x\text{TiO}_3$ thin films with $x = 0$ at 15 K (a), 30 K (b), 50 K (c), 70 K (d), 100 K (e) and 295 K (f) measured at 100 Hz.

Thus, P_r of all studied Bi-doped STO films is higher than that of undoped STO. P_r and E_c have the highest values for Bi content $x = 0.04$, with a decrease for the higher dopant content of $x = 0.10$. The smooth decrease of P_r and E_c with increasing temperature, observed for all of the SBiT films, is typical for relaxor ferroelectrics [71].

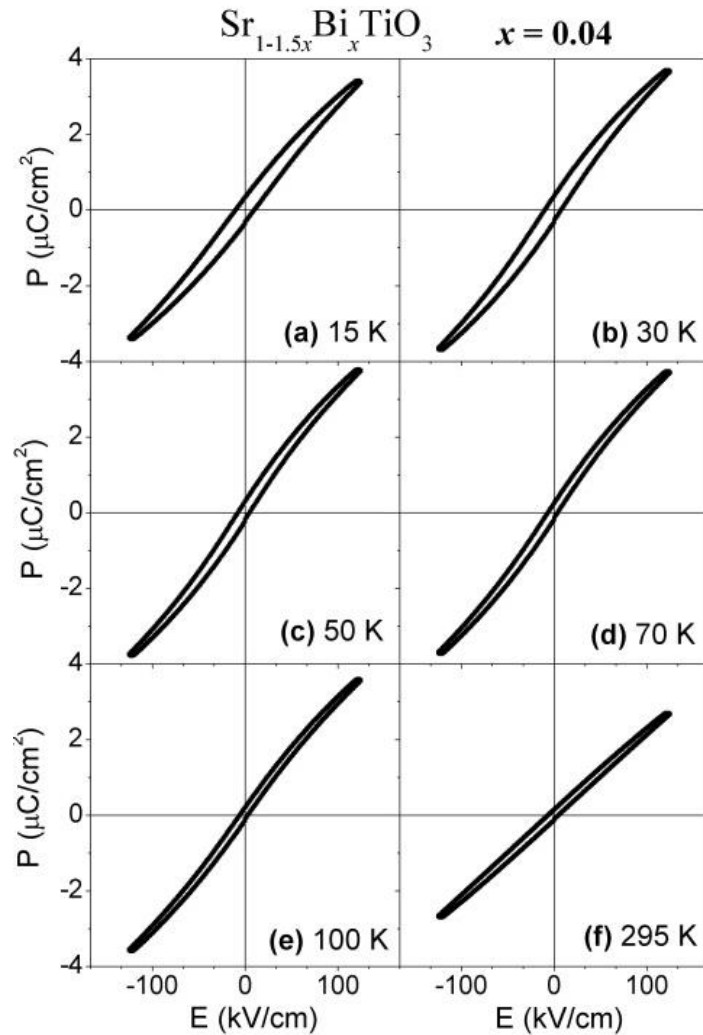


Figure 19. $P(E)$ hysteresis loops of $\text{Sr}_{1-1.5x}\text{Bi}_x\text{TiO}_3$ thin films with $x = 0.04$ at 15 K (a), 30 K (b), 50 K (c), 70 K (d), 100 K (e) and 295 K (f) measured at 100 Hz.

For SBiT ceramics, S -shape hysteresis loops with remanent polarisation $\sim 0.31 \mu\text{C}/\text{cm}^2$ for $x = 0.0033$, $\sim 0.83 \mu\text{C}/\text{cm}^2$ for $x = 0.0133$ and $\sim 0.32 \mu\text{C}/\text{cm}^2$ for $x = 0.0533$ at 11 K and 50 Hz were reported [12]. Similarly to the films of this study, as the Bi content increases in SBiT ceramics, a

slimmer hysteresis loop with low polarisation and without S-shape was observed, disappearing with the increase of temperature [10, 12].

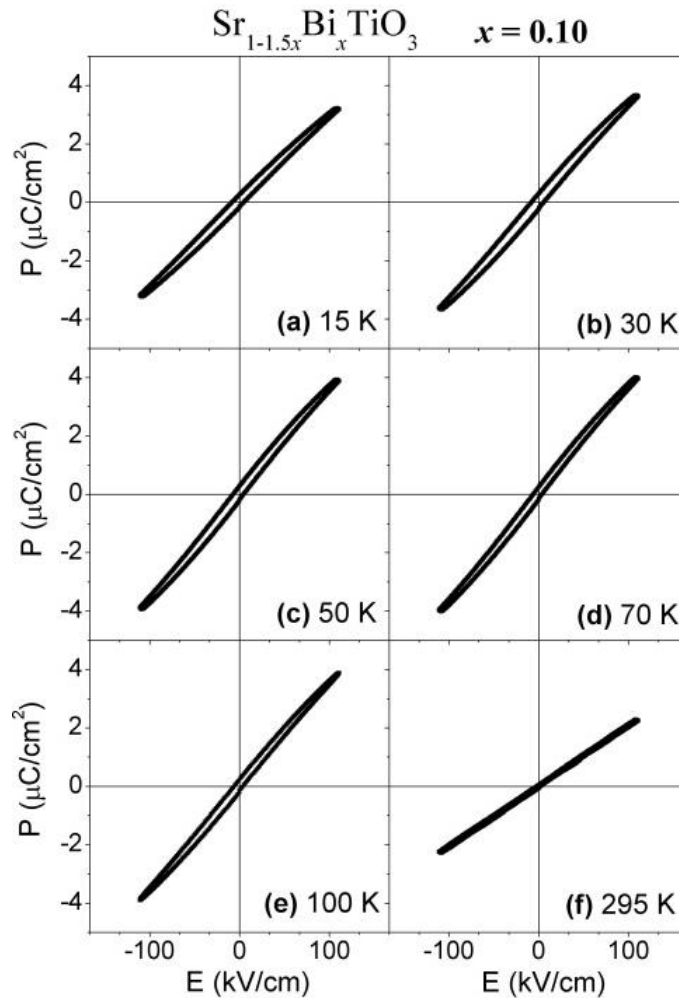


Figure 20. $P(E)$ hysteresis loops of $\text{Sr}_{1-1.5x}\text{Bi}_x\text{TiO}_3$ thin films with $x = 0.10$ at 15 K (a), 30 K (b), 50 K (c), 70 K (d), 100 K (e) and 295 K (f) measured at 100 Hz.

Thus, the main features typical for relaxors and SBiT ceramics as system with relaxor-like behaviour were also observed in $\text{Sr}_{1-1.5x}\text{Bi}_x\text{TiO}_3$ films:

- rounded peaks in the temperature dependence of ε' (Figure 11);
- temperature of the ε' peak always higher than the temperature of the loss peak (Figures 13 and 14);
- maximum of ε' decreases in value, and its temperature shifts to higher temperatures, with increasing measurement frequency (Figure 16);
- maximum of ε'' increases in value, and its temperature shifts to higher temperatures, with increasing measurement frequency (Figure 17);
- a compliance with a Vögel-Fulcher relation (Table 1);
- slim $P(E)$ hysteresis loops (Figures 18-20), etc.

Low-Temperature Dielectric Properties as a Function of dc Electric Field

The influence of an applied dc electric field on the dielectric response of $\text{Sr}_{1-1.5x}\text{Bi}_x\text{TiO}_3$ films was also addressed in our work. Figure 21 depicts the temperature dependence of the real part of dielectric permittivity ε' of $\text{Sr}_{1-1.5x}\text{Bi}_x\text{TiO}_3$ films with $x = 0, 0.0053, 0.04, 0.10$ and 0.167 , measured under $0, 25, 75$ and 125 kV/cm dc bias fields at a frequency of 10 kHz. As the applied dc electric field increases, the ε' of Bi-doped STO samples decreases, similar to undoped STO films. A maximum decrease of ε' is observed around the peak temperature. The highest influence of dc bias field on ε' is observed for SBiT films with $0.002 \leq x \leq 0.04$. Meanwhile, the dc electric field was reported to significantly suppress the peak in $\varepsilon'(T)$ of SBiT ceramics, with $x = 0.002, 0.0033$ and 0.0067 , induced by Bi incorporation [21, 23].

The relative tunability of SBiT thin films was calculated as:

$$n_r = [\varepsilon'(E_{dc} = 0) - \varepsilon'(E_{dc})]/\varepsilon'(E_{dc} = 0) \times 100\% \quad (3)$$

where $\varepsilon'(E_{dc} = 0)$ stands for the real part of dielectric permittivity at zero bias and, $\varepsilon'(E_{dc})$ for the real part of dielectric permittivity at the applied dc electric field [7].

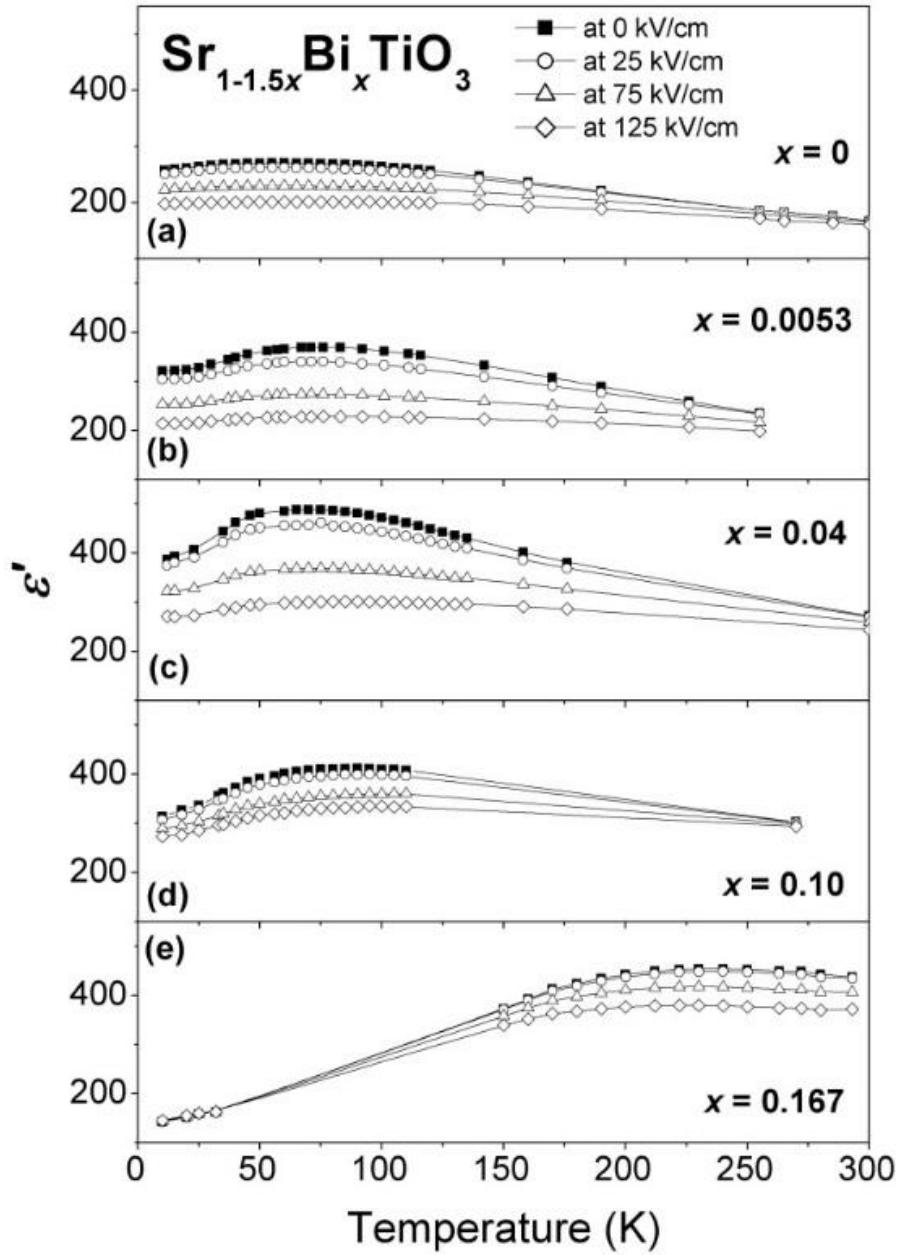


Figure 21. Variation of real part of the dielectric permittivity ϵ' of $\text{Sr}_{1-1.5x}\text{Bi}_x\text{TiO}_3$ thin films with $x = 0, 0.0053, 0.04, 0.10$ and 0.167 as a function of temperature under selected dc bias fields at 10 kHz.

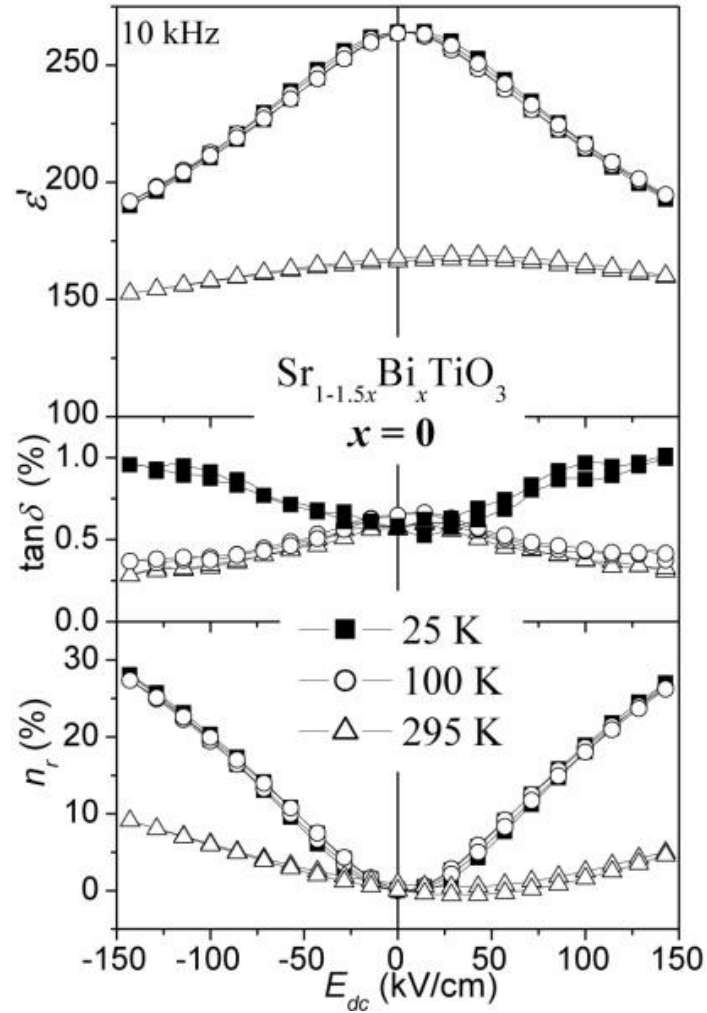


Figure 22. Variation of real part of the dielectric permittivity ϵ' (top panel), $\tan\delta$ (middle panel) and relative tunability n_r (bottom panel) of $\text{Sr}_{1-1.5x}\text{Bi}_x\text{TiO}_3$ thin films with $x = 0$ as a function of dc electric field at 10 kHz for selected temperatures.

The electric-field dependences of ϵ' , $\tan\delta$ and n_r of $\text{Sr}_{1-1.5x}\text{Bi}_x\text{TiO}_3$ films with $x = 0, 0.0053, 0.04, 0.10$ and 0.167 measured at 10 kHz in a dc field range of ± 150 kV/cm are presented in Figures 22, 23, 24, 25 and 26, respectively, for selected temperatures.

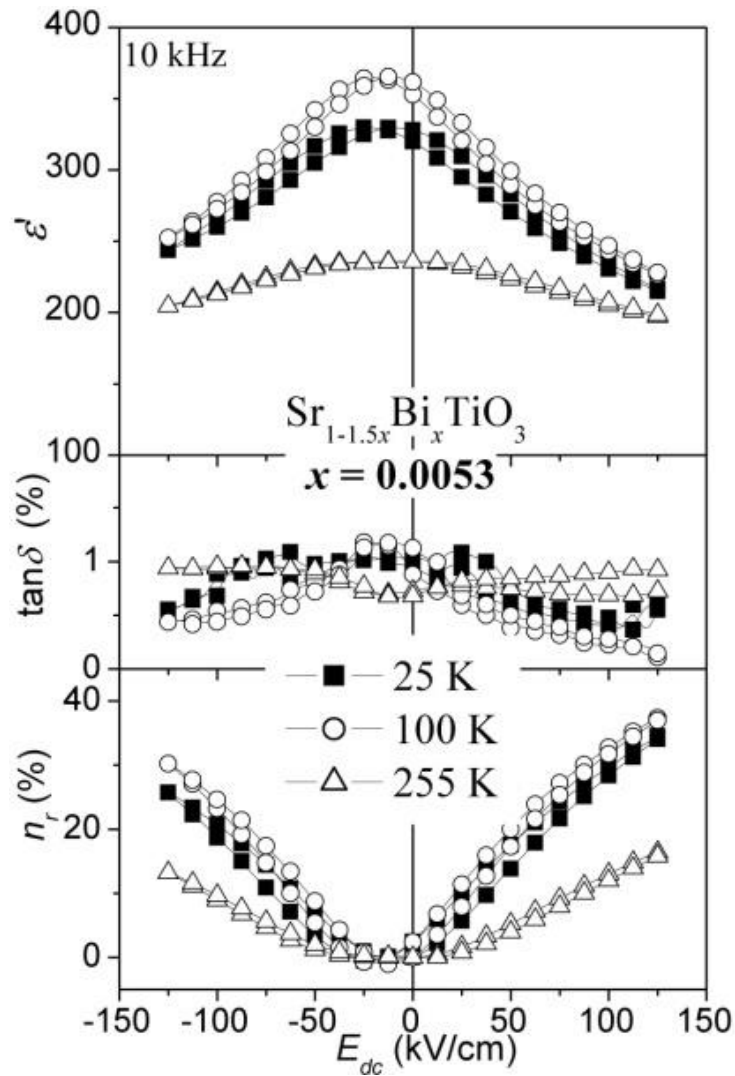


Figure 23. Variation of real part of the dielectric permittivity ϵ' (top panel), $\tan\delta$ (middle panel) and relative tunability n_r (bottom panel) of $\text{Sr}_{1-1.5x}\text{Bi}_x\text{TiO}_3$ thin films with $x = 0.0053$ as a function of dc electric field at 10 kHz for selected temperatures.

It is seen from Figures 22-26, that $\epsilon'(E_{dc})$, $\tan\delta(E_{dc})$ and $n_r(E_{dc})$ dependences strongly decrease with increasing Bi concentration. Their bell-like shape, observed at low temperatures for SBiT films with $x \leq 0.10$, suggests the presence of a polar phase.

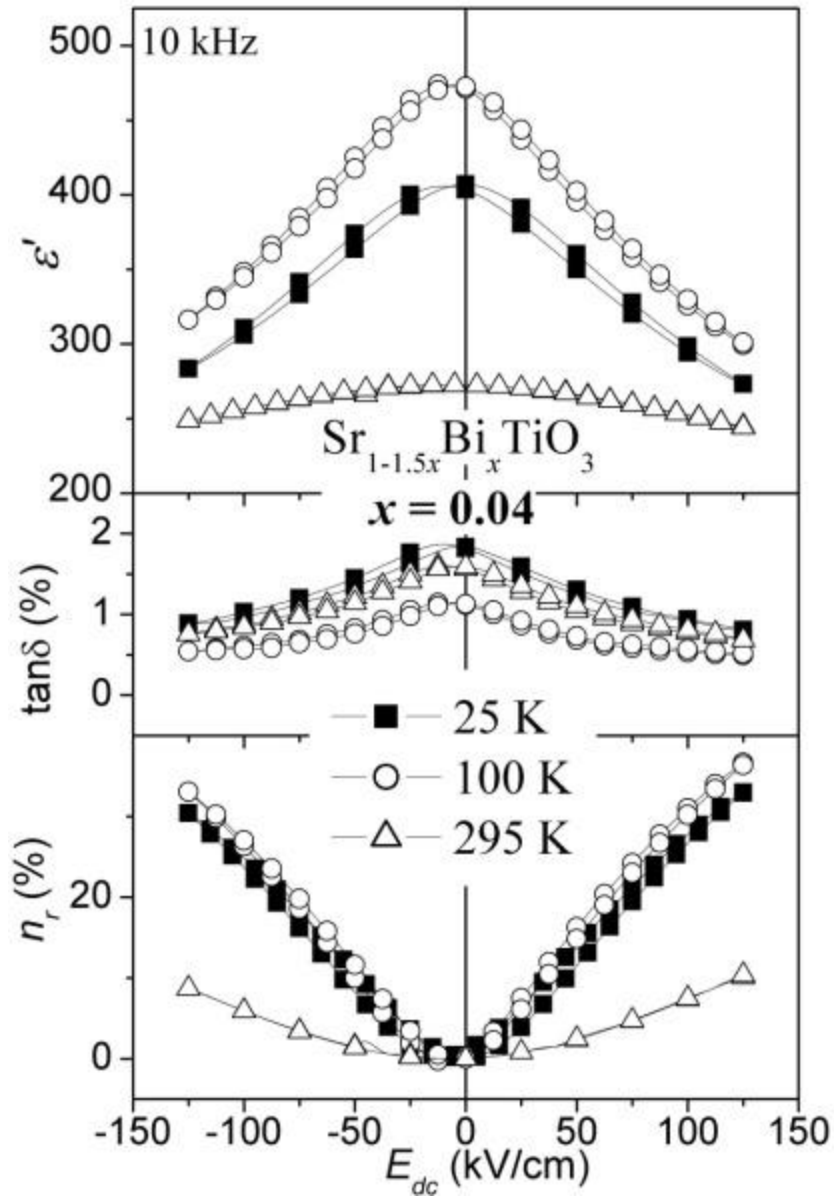


Figure 24. Variation of real part of the dielectric permittivity ϵ' (top panel), $\tan\delta$ (middle panel) and relative tunability n_r (bottom panel) of $\text{Sr}_{1-1.5x}\text{Bi}_x\text{TiO}_3$ thin films with $x = 0.04$ as a function of dc electric field at 10 kHz for selected temperatures.

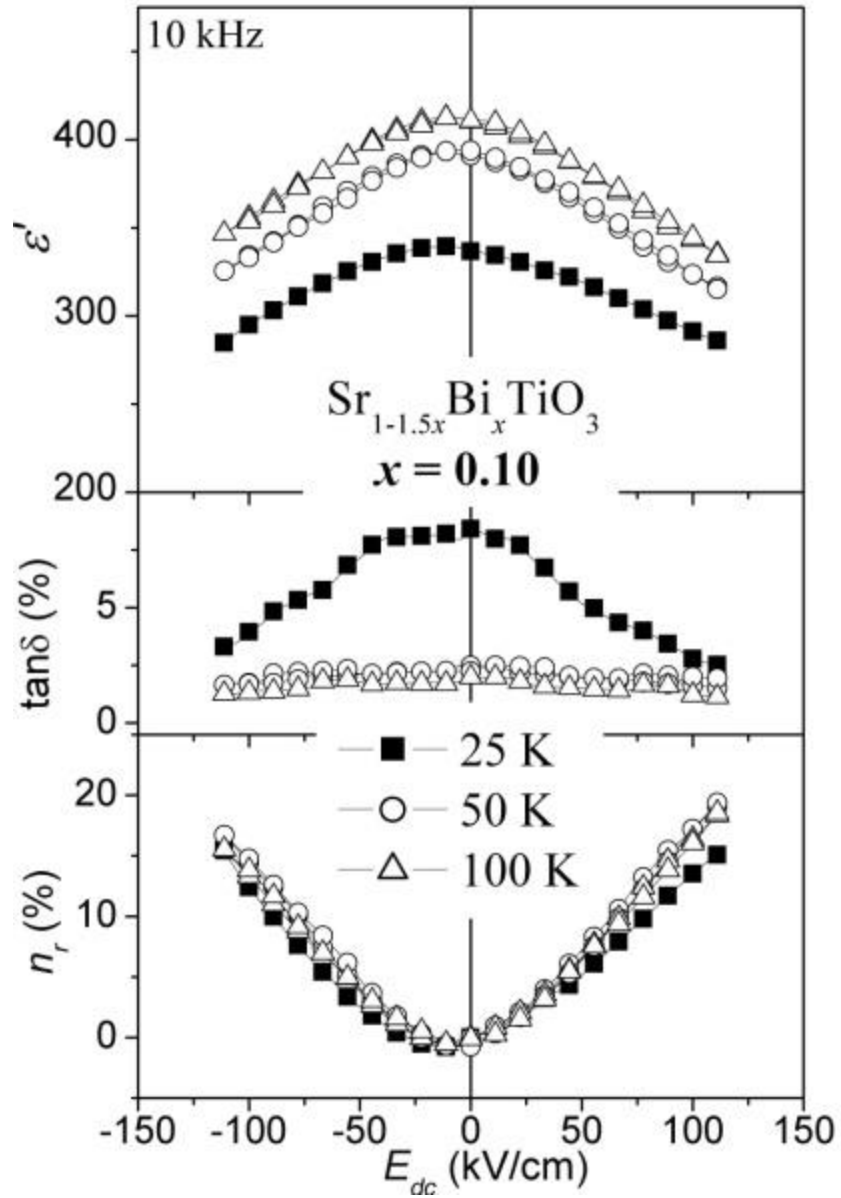


Figure 25. Variation of real part of the dielectric permittivity ϵ' (top panel), $\tan\delta$ (middle panel) and relative tunability n_r (bottom panel) of $\text{Sr}_{1-1.5x}\text{Bi}_x\text{TiO}_3$ thin films with $x = 0.10$ as a function of dc electric field at 10 kHz for selected temperatures.

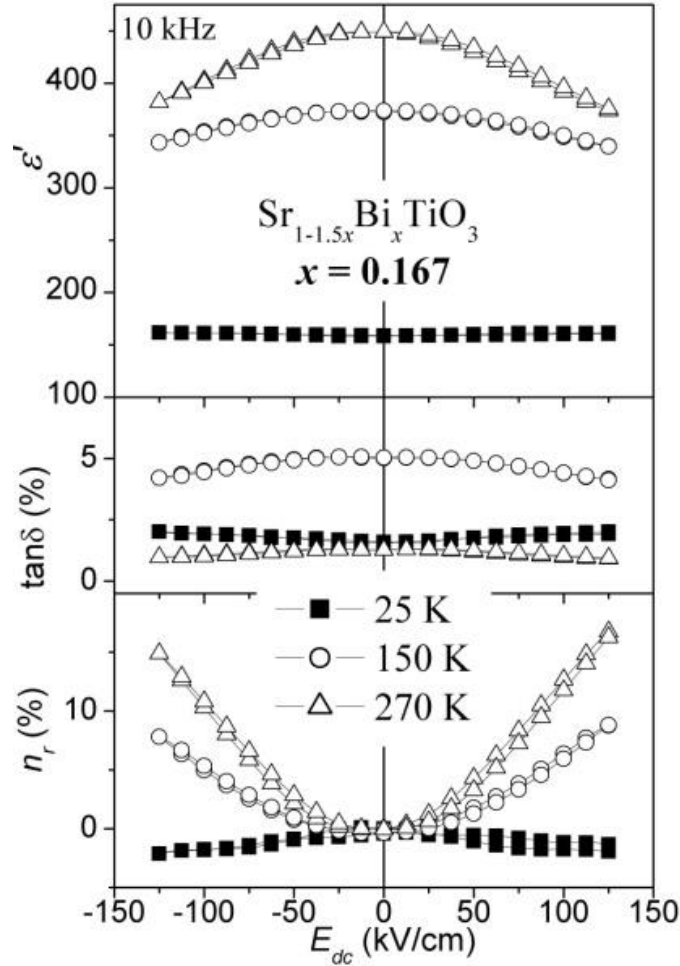


Figure 26. Variation of real part of the dielectric permittivity ϵ' (*top panel*), $\tan\delta$ (*middle panel*) and relative tunability n_r (*bottom panel*) of $\text{Sr}_{1-1.5x}\text{Bi}_x\text{TiO}_3$ thin films with $x = 0.167$ as a function of dc electric field at 10 kHz for selected temperatures.

The temperature dependence of the relative tunability n_r at 10 kHz and 125 kV/cm of Bi-doped STO films is presented in Figure 27. All SBiT films present a broad peak in $n_r(T)$, similar to that in $n_r(T)$ of undoped STO. This peak shifts with increasing Bi content, resembling that in $\epsilon'(T)$. Tunability of SBiT films with $x \leq 0.04$ is higher than that for undoped STO films ($\sim 25.6\%$ in the maximum at ~ 55 K) in all temperature ranges, and shows a

maximum value of $\sim 38.6\%$ at ~ 65 K for SBiT films with $x = 0.04$. With a further increase of Bi concentration ($x > 0.04$), n_r is smaller than that of undoped STO and SBiT films with small Bi content and the n_r maximum strongly shifts to high temperatures with increasing x : $\sim 20\%$ at ~ 60 K for $x = 0.10$, $\sim 16.7\%$ at ~ 253 K for $x = 0.167$.

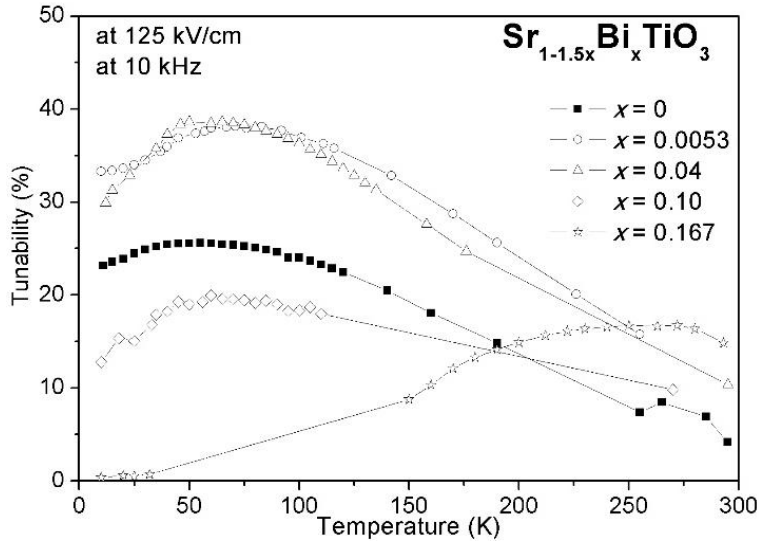


Figure 27. Temperature variation of the relative tunability n_r of $\text{Sr}_{1-1.5x}\text{Bi}_x\text{TiO}_3$ thin films at 125 kV/cm and 10 kHz.

To characterise these films in terms of possible tunable applications, the communication quality factor (K) was calculated, based on the following equation [47]:

$$K = \frac{(n-1)^2}{n \times \tan\delta(0) \times \tan\delta(E_{\max})} \quad (4)$$

where n stands for the tunability and can be calculated as $n = \varepsilon'(0)/\varepsilon'(E_{\max})$. K values of $\text{Sr}_{1-1.5x}\text{Bi}_x\text{TiO}_3$ thin films were calculated by Eq. (4) using data of $\varepsilon'(E)$ and $\tan\delta(E)$ at an applied dc -field of 125 kV/cm and frequency of 10 kHz, and are presented in Figure 28 as a function of the temperature.

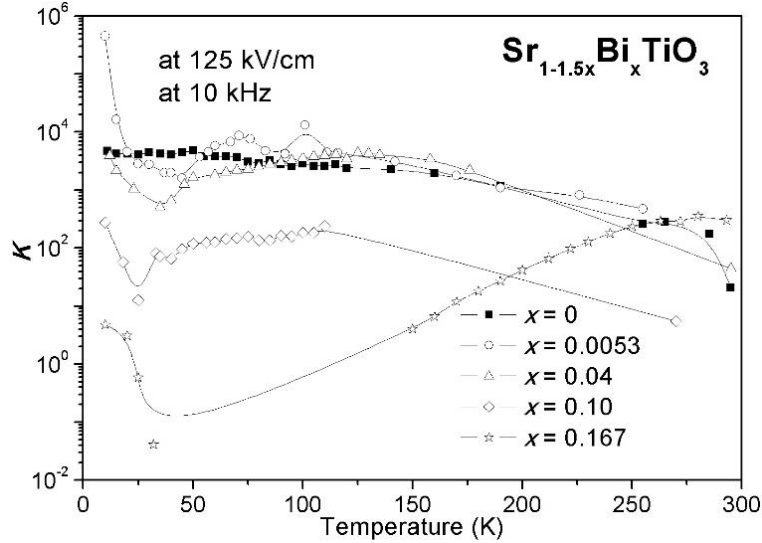


Figure 28. Temperature variation of communication quality factor K of $\text{Sr}_{1-1.5x}\text{Bi}_x\text{TiO}_3$ films at 125 kV/cm and 10 kHz.

It is obvious, that SBiT films with low Bi content $x \leq 0.04$ show similar or higher K than that of undoped STO from 50-100 K to room temperature. At the same time, SBiT films with high Bi content $x > 0.04$ present K values lower than that of undoped STO, due to the decrease of tunability and increase of $\tan\delta$. As claimed by Vendik et al., a tunable component with $K > 2000$ is suitable for practical application [47]. Thus, the analysed polycrystalline $\text{Sr}_{1-1.5x}\text{Bi}_x\text{TiO}_3$ films with $x \leq 0.04$ are all appropriate candidates for tunable applications.

CONCLUSION

Polycrystalline $\text{Sr}_{1-1.5x}\text{Bi}_x\text{TiO}_3$ ($x = 0 - 0.267$) films with thickness of ~ 450 nm, roughness less than 2 nm and average grain size from ~ 80 nm to ~ 120 nm were prepared by sol-gel, spin coated on Si/SiO₂/TiO₂/Pt substrates, and crystallised at 750°C. The solid solubility limit of Bi in STO thin films is $x = 0.167$, as determined by XRD. For higher Bi contents of $x \geq 0.267$,

$\text{Bi}_4\text{Ti}_3\text{O}_{12}$ appears as an extra-phase. Similar to $\text{Sr}_{1-1.5x}\text{Bi}_x\text{TiO}_3$ ceramics, the lattice parameter of SBIT films was found to increase with increasing Bi content. Expansion of the unit cell is explained by the slightly larger ionic size of $\text{Bi}_{(12)}^{3+}$ compared to that of the substituted $\text{Sr}_{(12)}^{2+}$ as well as by the formation of V_{Sr} and the corresponding electrostatic repulsion of adjacent oxygen anions.

$\epsilon'(T)$ of all $\text{Sr}_{1-1.5x}\text{Bi}_x\text{TiO}_3$ films revealed a strong rounded peak in the low frequency range. Moreover, strong frequency dispersion occurs, when ϵ'_{max} significantly decreases and shifts to the high temperature region with increasing frequency. Two peaks were induced in $\epsilon''(T)$, below the temperature of the peak in $\epsilon'(T)$ by Bi doping of STO films. Peak 1 was well observed at ~ 38 K in $\text{Sr}_{1-1.5x}\text{Bi}_x\text{TiO}_3$ films with $x \leq 0.10$, independent of Bi content, whereas peak 2 was clearly seen from ~ 68 K for films with $x = 0.0053$ to ~ 145 K for $x = 0.167$. All loss peaks of $\text{Sr}_{1-1.5x}\text{Bi}_x\text{TiO}_3$ films are frequency dependent. Additionally, the oxygen-vacancy related relaxation peak 3 was found to contribute to the dielectric losses of SBIT films. Furthermore, slim hysteresis loops of relaxor type were observed in SBIT films at low temperatures, implying the appearance of a polar state. Thus, the effect of Bi incorporation in STO films is qualitatively the same as the relaxor-like behaviour observed for Bi-doped STO ceramics, differing only in details.

Based on the tunability values (a maximum $\sim 38.62\%$ at ~ 65 K for SBIT films with $x = 0.04$) and quality factor values, the analysed polycrystalline $\text{Sr}_{1-1.5x}\text{Bi}_x\text{TiO}_3$ films with $x \leq 0.04$ prepared by sol-gel can be considered as promising materials for tunable device applications.

ACKNOWLEDGMENTS

This work was developed within the scope of the project CICECO-Aveiro Institute of Materials, FCT Ref. UID/CTM/50011/2019, financed by national funds through the FCT/MCTES as well as within FCT independent

researcher grant IF/00602/2013. Thanks to Dr. R. C. Pullar who assisted with the English language of this chapter.

REFERENCES

- [1] Rohrer, H. 1996. "The Nanoworld: Chances and Challenges." *Microelectron. Eng.* 32:5-14.
- [2] Song, Y., Yoo, D., Lee, T. 2018. "Miniaturization and Integration of Organic Resistive Memory Devices." *J. Korean Phys. Soc.* 73:479-487.
- [3] Zhang, P., Wang, F., Yu, M., Zhuang, X., Feng, X. 2018. "Two-dimensional Materials for Miniaturized Energy Storage Devices: from Individual Devices to Smart Integrated Systems." *Chem. Soc. Rev.* 47:7426-7451.
- [4] Morita T. 2003. "Miniature Piezoelectric Motors." *Sens. Actuator A-Phys.* 103:291-300.
- [5] Alzahrani, S., Kalkur, T., Song, H. 2014. "A Frequency Agile Miniaturized Antenna Utilizing Ferroelectric Barium-Strontium-Titanate Capacitors." *MRS Proc.* (2012) 1691:mrss14-1691-bb11-35.
- [6] Acikel, B., Taylor, T. R., Hansen, P. J., Speck, J. S., York, R. A. 2002. "A New High Performance Phase Shifter using (Ba,Sr)TiO₃ Thin Films." *IEEE Microw. Wirel. Compon. Lett.* 12:237-239.
- [7] Tagantsev, A. K., Sherman, V. O., Astafiev, K. F., Venkatesh, J., Setter, N. J. 2003. "Ferroelectric Materials for Microwave Tunable Applications." *J. Electroceram.* 11:5-66.
- [8] Skanavi, G. I., Ksendzov, I. J., Trigubenko, V. A., Prokhvatilov, V. G. 1957. "Relaxation Polarization and Losses in Nonferroelectric Dielectrics with High Dielectric Constants." *Zh. Eksp. Teor. Fiz.* 33:320-334 [1958. *Sov. JETP* 6:250-259].
- [9] Smolenskii, G. A., Isupov, V. A., Agranovskaya, A. A., Popov, S. N. 1960 "Ferroelectrics with Diffuse Phase Transitions." *Fiz. Tverd. Tela* 2:2906-2918 [1961. *Sov. Phys. Solid State* 2:2584-2594].

- [10] Yu, Z., Ang, C., Vilarinho, P. M., Mantas, P. Q., Baptista, J. L. 1998. "Dielectric Relaxation Behaviour of Bi:SrTiO₃: I. The Low Temperature Permittivity Peak." *J. Eur. Ceram. Soc.* 18:1613-1619.
- [11] Yu, Z., Ang, C., Vilarinho, P. M., Mantas, P. Q., Baptista J. L. 1998. "Dielectric Relaxation Behaviour of Bi:SrTiO₃: II. Influence of Heat Treatment on Dielectric Properties." *J. Eur. Ceram. Soc.* 18:1621-1628.
- [12] Ang, C., Yu, Z., Vilarinho, P. M., Baptista, J. L. 1998. "Bi:SrTiO₃: A Quantum Ferroelectric and a Relaxor." *Phys. Rev. B* 57:7403-7406.
- [13] Ang, C., Scott, J. F., Yu, Z., Ledbetter, H., Baptista, J. L. 1999. "Dielectric and Ultrasonic Anomalies at 16, 37, and 65 K in SrTiO₃." *Phys. Rev. B* 59:6661-6664.
- [14] Ang, C., Yu, Z., Hemberger, J., Lunkenheimer, P., Loidl, A. 1999. "Dielectric Anomalies in Bismuth-doped SrTiO₃: Defect Modes at Low Impurity Concentrations." *Phys. Rev. B* 59:6665-6669.
- [15] Ang, C., Yu, Z., Lunkenheimer, P., Hemberger, J., Loidl, A. 1999. "Dielectric Relaxation Modes in Bismuth-doped SrTiO₃: The Relaxor Behaviour." *Phys. Rev. B* 59:6670-6674.
- [16] Ang, C., Yu, Z., Zhi, J. 2000. "Impurity-induced Ferroelectric Relaxor Behavior in Quantum Paraelectric SrTiO₃ and Ferroelectric BaTiO₃" *Phys. Rev. B* 61:957-961.
- [17] Ang, C., Yu, Z. 2000. "Phonon-coupled Impurity Dielectric Modes in Sr_{1-1.5x}Bi_xTiO₃." *Phys. Rev. B* 61:11363-11366.
- [18] Ang, C., Yu, Z., Cross, L. E. 2000. "Oxygen-vacancy-related Low-frequency Dielectric Relaxation and Electrical Conduction in Bi:SrTiO₃." *Phys. Rev. B* 62:228-236.
- [19] Ang, C, Yu, Z., Scott, J., Loidl, A., Guo, R., Bhalla, A. S., Cross, L. E. 2000. "Dielectric Polarization Processes in Bi:SrTiO₃." *J. Phys. Chem. Solids* 61:191-196.
- [20] Yu, Z., Ang, C., Guo, R., Bhalla, A. S., Cross, L. E. 2001. "Oxygen Vacancy Related Dielectric Relaxation in (Sr_{1-1.5x}Bi_x)TiO₃." *Ferroelectrics* 262:219-225.
- [21] Ang, C., Yu, Z. 2002. "Dielectric Relaxor and Ferroelectric Relaxor: Bi-doped Paraelectric SrTiO₃." *J. Appl. Phys.* 91:1487-1494.

- [22] Yu, Z., Ang, C. 2003. "Crystalline Structure and Dielectric Properties of $(\text{Sr}_{1-1.5x}\text{Bi}_x)\text{TiO}_3$ Ceramics." *J. Mater. Sci.* 38:113-118.
- [23] Ang, C., Yu, Z. 2004. "dc Electric-field Dependence of the Dielectric Constant in Polar Dielectrics: Multipolarization Mechanism Model." *Phys. Rev. B* 69:1741109.
- [24] Okhay, O., Bergano, V. M. X., Wu, A., Vilarinho, P. M. 2006. "Bi Effect on the Microstructure and Dielectric Properties of SrTiO_3 Thin Films." *Mater. Sci. Forum* 514-516:245-249.
- [25] Zhao, M., Yao, X., Shi, P., Wie, X., Wu, X., Ren, W., Lin, P. 2008. "Effect of Poly(vinyl acetate) on Structure and Property of Bismuth-doped Strontium Titanate Thin Films Derived by Sol-gel Method." *Ceram. Int.* 34:997-1001.
- [26] Shi, P., Ren, W., Zhao, M., Wei, X., Wu, X., Chen, X., Yao, X. 2009. "Structure and Dielectric Properties of $(\text{Sr}_{1-1.5x}\text{Bi}_x)\text{TiO}_3$ Thin Films." *J. Appl. Phys.* 105:084104.
- [27] Okhay, O., Wu, A., Vilarinho, P. M., Tkach, A. 2010. "Dielectric Response of Polycrystalline $\text{Sr}_{1-1.5x}\text{Bi}_x\text{TiO}_3$ Thin Films under Direct Current Bias." *Appl. Phys. Lett.* 97:062912.
- [28] Okhay, O., Wu, A., Vilarinho, P. M., Tkach, A. 2011. "Dielectric Relaxation of $\text{Sr}_{1-1.5x}\text{Bi}_x\text{TiO}_3$ Sol-gel Thin Films." *J. Appl. Phys.* 109:064103.
- [29] Müller, K. A., Burkard, H. 1979. " SrTiO_3 - An Intrinsic Quantum Paraelectric below 4 K." *Phys. Rev. B* 19:3593-3602
- [30] Lemanov, V. V., Sotnikov, A. V., Smirnova, E. P., Weihnacht, M., Kunze, R. 1999. Perovskite CaTiO_3 as an Incipient Ferroelectric *Solid State Commun.* 110:611-614.
- [31] Barrett, J. H. 1952. "Dielectric Constant in Perovskite type Crystals." *Phys. Rev.* 86:118-120.
- [32] Viana, R., Lunkenheimer, P., Hemberger, J., Bohmer, R., Loidl, A. 1994. "Dielectric Spectroscopy in SrTiO_3 ." *Phys. Rev. B* 52:601-604.
- [33] Dec, J., Kleemann, W., Westwanski, B. 1999. "Scaling Behaviour of Strontium Titanate." *J. Phys.: Condens. Matter.* 11:L379-L384.

- [34] Venturini, E. L., Samara, G. A., Itoh, M., Wang, R. 2004. "Pressure as a Probe of the Physics of ^{18}O -substituted SrTiO_3 ." *Phys. Rev. B* 69:184105.
- [35] Mizaras, R., Loidl, A. 1997. "Central Peak in SrTiO_3 Studied by Dielectric Spectroscopy." *Phys. Rev. B* 56:10726-10729.
- [36] Abe, K., Komatsu, S. 1993. "Measurement and Thermodynamic Analyses of the Dielectric Constant of Epitaxially Grown SrTiO_3 Films." *Jpn. J. Appl. Phys.* 32:L1157-L1159.
- [37] Dietz, G. W., Antpohler, W., Klee, M., Waser, R. 1995. "Electrode Influence on the Charge Transport through SrTiO_3 Thin Films." *J. Appl. Phys.* 78, 6113-6121.
- [38] Dietz, G. W., Waser, R. 1997. "Charge Injection in SrTiO_3 Thin Films." *Thin Solid Films* 299:53-58.
- [39] Bascieri, C., Strieffer, S. K., Kingon, A. I., Waser, R. 1997. "The Dielectric Response as a Function of Temperature and Film Thickness of Fiber-textured $(\text{Ba,Sr})\text{TiO}_3$ Thin Films Grown by Chemical Vapor Deposition." *J. Appl. Phys.* 82:2497-2504.
- [40] Li, H.-C., Si, W., West, A. D., Xi, X. X. 1998. "Thickness Dependence of Dielectric Loss in SrTiO_3 Thin Films." *Appl. Phys. Lett.* 73:464-466.
- [41] Tkach, A., Okhay, O., Vilarinho, P. M., Kholkin, A. L. 2008. "High Dielectric Constant and Tunability of Strontium Titanate Ceramics Modified by Chromium Doping." *J. Phys.: Condens. Matter* 20:415224.
- [42] Findikoglu, A. T., Doughty, C., Anlage, S. M., Li, Q., Xi, X. X., Venkatesana, T. 1993. "Effect of dc Electric Field on the Effective Microwave Surface Impedance of $\text{YBa}_2\text{Cu}_3\text{O}_7/\text{SrTiO}_3/\text{YBa}_2\text{Cu}_3\text{O}_7$ Trilayers." *Appl. Phys. Lett.* 63:3215-3217.
- [43] Astafiev, K., Sherman, V., Tagantsev, A., Setter, N., Petrov, P., Kaydanova, T., Ginley, D., Hoffmann-Eifert, S., Bottger, U., Waser, R. 2003. "Shift of Phase Transition Temperature in Strontium Titanate Thin Films." *Integr. Ferroelectr.* 59:1371-1379.
- [44] Yamada, T., Astafiev, K., Sherman, V., Tagantsev, A., Muralt, P., Setter, N. 2005. "Strain Relaxation of Epitaxial SrTiO_3 Thin Films on

- LaAlO₃ by Two-step Growth Technique.” *Appl. Phys. Lett.* 86:142904.
- [45] Li, H.-C., Si, W., West, A. D., Xi, X. X. 1998. “Near Single Crystal-level Dielectric Loss and Nonlinearity in Pulsed Laser Deposited SrTiO₃ Thin Films.” *Appl. Phys. Lett.* 73:190-192.
- [46] Keane, S. P., Schmidt, S., Lu, J., Romanov, A. E., Stemmer, S. 2006. “Phase Transitions in Textured SrTiO₃ Thin Films on Epitaxial Pt Electrodes.” *J. Appl. Phys.* 99:033521.
- [47] Vendik, O. G., Hollmann, E. K., Kozyrev, A. B., Prudan, A. M. 1999. “Ferroelectric Tuning of Planar and Bulk Microwave Devices.” *J. Supercond.* 12:325-338.
- [48] Shannon, R. D. 1976. “Revised Effective Ionic Radii and Systematic Studies of Interatomic Distances in Halides and Chalcogenides.” *Acta Cryst. A* 32:751-767.
- [49] Lemanov, V. V. 1999. “Phase Transitions in SrTiO₃ Quantum Paraelectric with Impurities.” *Ferroelectrics* 226:133-146.
- [50] Tkach, A., Vilarinho, P. M., Kholkin A. 2004. “Structural and Dielectric Properties of Mn-doped Strontium Titanate Ceramics”, *Ferroelectrics* 304:87-90.
- [51] Bednorz, J. G., Müller, K. A. 1984. “Sr_{1-x}Ca_xTiO₃: An XY Quantum Ferroelectric with Transition to Randomness.” *Phys. Rev. Lett.* 52:2289-2292.
- [52] Zhang, L., Kleemann, W., Zhong, W.-L. 2002. “Relation Between Phase Transition and Impurity-polarized Clusters in Sr_{1-β}Ca_βTiO₃.” *Phys. Rev. B* 66:104105.
- [53] Ranjan, R., Pandey, D., Lalla, N. P. 2000. “Novel Features of Sr_{1-x}Ca_xTiO₃ Phase Diagram: Evidence for Competing Antiferroelectric and Ferroelectric Interactions.” *Phys. Rev. Lett.* 84:3726-3729.
- [54] Hirata, T., Ishioka, K., Kitajima, M. 1996. “Vibrational Spectroscopy and X-Ray Diffraction of Perovskite Compounds Sr_{1-x}M_xTiO₃ (M = Ca, Mg; 0 ≤ x ≤ 1).” *J. Solid State Chem.* 124:353-359.
- [55] Lemanov, V. V., Smirnova, E. R., Syrikov, P. P., Tarakanov, E. A. 1996. “Phase Transitions and Glasslike Behavior in Sr_{1-x}Ba_xTiO₃.” *Phys. Rev. B* 54:3151-3157.

- [56] Ostapchuk, T., Petzelt, J., Kužel, P., Veljko, S., Tkach, A., Vilarinho, P., Ponomareva, I., Bellaiche, L., Smirnova, E., Lemanov, V., Sotnikov, A., Weihnacht, M. 2008. "Infrared and THz Soft-mode Spectroscopy of (Ba,Sr)TiO₃ Ceramics." *Ferroelectrics* 367:139-148.
- [57] Smirnova, E. P., Sotnikov, A. V., Kunze, R., Weihnacht, M., Kvyatkovskii, O. E., Lemanov, V. V. 2005. "Interrelation of Antiferrodistortive and Ferroelectric Phase Transitions in Sr_{1-x}A_xTiO₃ (A = Ba, Pb)." *Solid State Commun.* 133:421-425.
- [58] Guzhva, M. E., Lemanov, V. V., Markovin, P. A., Shuplygina, T. A. 1998. "Ferroelectric Behaviour and Phase Diagrams of SrTiO₃-based Solid Solutions." *Ferroelectrics* 218:93-101.
- [59] Tkach, A., Vilarinho, P. M., Kholkin, A. 2005. "Polar Behavior in Mn-doped SrTiO₃ Ceramics." *Appl. Phys. Lett.* 86:172902.
- [60] Tkach, A., Vilarinho, P. M., Kholkin, A. L. 2005. "Structure-Microstructure-Dielectric Tunability Relationship in Mn-doped Strontium Titanate Ceramics." *Acta Mater.* 53:5061-5069.
- [61] Tkach, A., Vilarinho, P. M., Kholkin, A. L., Pashkin, A., Veljko, S., Petzelt, J. 2006. "Broad-band Dielectric Spectroscopy Analysis of Relaxational Dynamics in Mn-doped SrTiO₃ Ceramics." *Phys. Rev. B* 73:104113.
- [62] Tkach, A., Vilarinho, P. M., Kholkin, A. L. 2006. "Dependence of Dielectric Properties of Manganese-doped Strontium Titanate Ceramics on Sintering Atmosphere." *Acta Mater.* 54:5385-5391.
- [63] Tkach, A., Vilarinho, P. M., Kholkin, A. L. 2007. "Nonlinear dc Electric-field Dependence of the Dielectric Permittivity and Cluster Polarization of Sr_{1-x}Mn_xTiO₃ Ceramics." *J. Appl. Phys.* 101:084110.
- [64] Johnson, D. W., Cross, L. E., Hummel, F. A. 1970. "Dielectric Relaxation in Strontium Titanates Containing Rare-Earth Ions." *J. Appl. Phys.* 41:2828-2833.
- [65] Iguchi, E., Lee, K. J. 1993. "Dielectric Relaxations in SrTiO₃ Doped with La₂O₃ and MnO₂ at Low Temperatures." *J. Mater. Sci.* 28:5809-5813.

- [66] Wang, R., Inaguma, Y., Itoh, M. 2000. "Predominant Factors for Quantum Paraelectric-Quantum Ferroelectric Transition in SrTiO₃-based Oxides." *Physica B* 284-288:1141-1142.
- [67] Tkach, A., Amaral, J. S., Amaral, V. S., Vilarinho, P. M. 2017. "Dielectric Spectroscopy and Magnetometry Investigation of Gd-doped Strontium Titanate Ceramics." *J. Eur. Ceram. Soc.* 37:2391-2397.
- [68] Tkach, A., Amaral, J. S., Zlotnik, S., Amaral, V. S., Vilarinho, P.M. 2018. "Enhancement of the Dielectric Permittivity and Magnetic Properties of Dy Substituted Strontium Titanate Ceramics." *J. Eur. Ceram. Soc.* 38:605-611.
- [69] Tkach, A., Vilarinho, P. M., Almeida, A. 2015. "Low-temperature Dielectric Relaxations in Y-doped Strontium Titanate Ceramics." *J. Phys. D: Appl. Phys.* 48:085302.
- [70] Tkach, A., Okhay, O., Almeida, A., Vilarinho, P. M. 2017. "Giant Dielectric Permittivity and High Tunability in Y-doped SrTiO₃ Ceramics Tailored by Sintering Atmosphere." *Acta Mater.* 130:249-260.
- [71] Smolenskii, G. A. 1984. *Ferroelectrics and Related Materials*. New York: Gordon and Breach Science Publishers.
- [72] Porokhonsky, V., Pashkin, A., Bovtun, V., Petzelt, J., Savinov, M., Samoukhina, P., Ostapchuk, T., Pokorny, J., Avdeev, M., Kholkin, A., Vilarinho, P. "Broad-band Dielectric Spectroscopy of SrTiO₃:Bi Ceramics." 2004. *Phys. Rev. B* 69:144104.
- [73] Bovtun, V., Porokhonsky, V., Savinov, M., Pashkin, A., Zelezny, V., Petzelt, J. 2004. "Broad-band Dielectric Response of Doped Incipient Ferroelectrics." *J. Eur. Ceram. Soc.* 24:1545-1549.
- [74] Smolenskii, G. A. 1970. "Physical Phenomena in Ferroelectrics with Diffused Phase Transition." *J. Phys. Soc. Jpn* 28:26-37.
- [75] Cross, L. E. 1994. "Relaxor Ferroelectrics: An Overview." *Ferroelectrics* 151:305-320.
- [76] Bovtun, V., Petzelt, J., Porokhonsky, V., Kamba, S., Yakimenko, Y. 2001. "Structure of the Dielectric Spectrum of Relaxor Ferroelectrics." *J. Eur. Ceram. Soc.* 21:1307-1311.

- [77] Frohlich, H. 1958. *Theory of Dielectrics*. London:Oxford University Press.
- [78] Viehland, D., Lang, S. J., Cross, L. E., Wuttig, M. 1990. "Freezing of the Polarization Fluctuations in Lead Magnesium Niobate Relaxors." *J. Appl. Phys.* 68:2916-2921.
- [79] Tkach, A., Correia, T. M., Almeida, A., Agostinho Moreira, J., Chaves, M. R. Okhay, O., Vilarinho, P. M., Gregora, I., Petzelt, J. 2011. "Role of Trivalent Sr-Substituents and Sr-vacancies in Tetragonal and Polar States of SrTiO₃." *Acta Mater.* 59:5388-5397.
- [80] Tkach, A., Almeida, A., Agostinho Moreira, J., Correia, T. M., Chaves, M. R. Okhay, O., Vilarinho, P. M., Gregora, I., Petzelt, J. 2011. "Enhancement of Tetragonality and Role of Strontium Vacancies in Heterovalent Doped SrTiO₃." *Appl. Phys. Lett.* 98:052903.
- [81] Yu, Z., Ang, C., Guo, R., Bhalla, A. S., Cross, L.E. 2002. "Dielectric Loss Modes of SrTiO₃ Thin Films Deposited on Different Substrates." *Appl. Phys. Lett.* 80:1034-1036.
- [82] Okhay, O., Tkach, A., Wu, A., Vilarinho, P. M. 2013. "Manipulation of the Dielectric Permittivity of Sol-gel SrTiO₃ Thin Films by Deposition Conditions." *J. Phys. D: Appl. Phys.* 46:505315.